AGU PUBLICATIONS

JGR

Journal of Geophysical Research: Earth Surface

RESEARCH ARTICLE
10.1002/2016JF004121

Key Points:
- Modeling and field data combined to determine LGM ice sheet extent in the SE Weddell Sea embayment
- Ice was not grounded at the continental shelf break for a prolonged period during the LGM
- Ocean and ice shelf processes play an important role in determining ice sheet stability

Supporting Information:
- Supporting Information S1
- Table S1
- Table S2
- Table S3
- Movie S1
- Movie S2
- Movie S3
- Movie S4
- Movie S5
- Movie S6

Correspondence to:
P. L. Whitehouse,
pippa.whitehouse@durham.ac.uk

Citation:
Whitehouse, P. L., M. J. Bentley, A. Vieli, S. S. R. Jamieson, A. S. Hein, and D. E. Sugden (2017), Controls on Last Glacial Maximum ice extent in the Weddell Sea embayment, Antarctica, *J. Geophys. Res. Earth Surf.*, *122*, doi:10.1002/2016JF004121.

Received 24 OCT 2016
Accepted 14 DEC 2016
Accepted article online 16 DEC 2016

Controls on Last Glacial Maximum ice extent in the Weddell Sea embayment, Antarctica

Pippa L. Whitehouse[1], Michael J. Bentley[1], Andreas Vieli[2], Stewart S. R. Jamieson[1], Andrew S. Hein[3], and David E. Sugden[3]

[1]Department of Geography, Durham University, Durham, UK, [2]Department of Geography, University of Zurich, Zurich, Switzerland, [3]School of GeoSciences, University of Edinburgh, Edinburgh, UK

Abstract The Weddell Sea sector of the Antarctic Ice Sheet is hypothesized to have made a significant contribution to sea-level rise since the Last Glacial Maximum. Using a numerical flowline model we investigate the controls on grounding line motion across the eastern Weddell Sea and compare our results with field data relating to past ice extent. Specifically, we investigate the influence of changes in ice temperature, accumulation, sea level, ice shelf basal melt, and ice shelf buttressing on the dynamics of the Foundation Ice Stream. We find that ice shelf basal melt plays an important role in controlling grounding line advance, while a reduction in ice shelf buttressing is found to be necessary for grounding line retreat. There are two stable positions for the grounding line under glacial conditions: at the northern margin of Berkner Island and at the continental shelf break. Global mean sea-level contributions associated with these two scenarios are ~50 mm and ~130 mm, respectively. Comparing model results with field evidence from the Pensacola Mountains and the Shackleton Range, we find it unlikely that ice was grounded at the continental shelf break for a prolonged period during the last glacial cycle. However, we cannot rule out a brief advance to this position or a scenario in which the grounding line retreated behind present during deglaciation and has since re-advanced. Better constraints on past ice sheet and ice shelf geometry, ocean temperature, and ocean circulation are needed to reconstruct more robustly past behavior of the Foundation Ice Stream.

1. Introduction

The extent to which grounded ice of the West Antarctic Ice Sheet expanded into the Weddell Sea during the last glacial cycle is one of the most poorly constrained aspects of recent Antarctic history [e.g., *Bentley et al.*, 2014; *Hillenbrand et al.*, 2014]. There remain unanswered questions regarding both the magnitude and timing of grounding line advance and retreat [*Anderson et al.*, 2002], and the contribution of this sector to global sea-level rise since the Last Glacial Maximum (LGM) [*Bentley*, 1999]. Crucially, this latter factor depends on both the extent and the thickness of the LGM ice sheet. If the LGM grounding line in the Weddell Sea reached the continental shelf break this would have increased the area of grounded West Antarctic ice by ~45% compared with today. However, if this expanded ice sheet were relatively thin and hence close to flotation, then the net effect on global mean sea level would have been minimal. It is therefore important to understand the past thickness and dynamics of this portion of the ice sheet.

It has been hypothesized that the rapid deglaciation of marine-based sectors of West Antarctica may have contributed to meltwater pulse 1A (MWP-1A), an ~300-year period of accelerated (>40 mm/yr) sea-level rise around 14,600 years ago [*Clark et al.*, 2009; *Deschamps et al.*, 2012]. While onshore evidence for such a rapid, coherent decrease in Antarctic ice volume remains elusive [*Bentley et al.*, 2010; *Hall et al.*, 2015], there is evidence for an increase in the flux of ice-rafted debris close to the Antarctic Peninsula around the time of MWP-1A [*Weber et al.*, 2014]. This raises the question of whether there could have been a re-organization of the marine-based or floating sectors of the ice sheet during deglaciation without significant onshore thinning. One process that can trigger rapid grounding line retreat of an ice sheet close to flotation is the marine ice sheet instability [*Thomas and Bentley*, 1978; *Weertman*, 1974], which arises because ice flux increases nonlinearly with respect to ice thickness at the grounding line [*Schoof*, 2007]. Such a process is facilitated if the bed beneath the ice deepens inland; this is the case across much of the Weddell Sea, making this sector susceptible to unstable grounding line retreat (or advance), both in the past and at present [*Joughin and Alley*, 2011; *Ross et al.*, 2012]. However, there are other factors that must be taken into consideration in order to understand the dynamics of this region, including (i) the stabilizing effect of the Filchner-Ronne Ice Shelf [*Gudmundsson*, 2013] and the role of the ocean in governing its past configuration

[*Kusahara et al*., 2015]; (ii) changes to the mass balance of the region, for example, due to changes in accumulation or ice stream configuration; and (iii) the potential stabilizing effect of processes associated with glacial isostatic adjustment (GIA) [*Gomez et al*., 2010; *Greischar and Bentley*, 1980] or ice rise development [*Matsuoka et al*., 2015].

The profile and maximum extent of the Antarctic Ice Sheet in the western portion of the Weddell Sea embayment have previously been constrained by using data relating to past ice thickness in the Ellsworth Mountains [*Bentley et al*., 2010; *Hein et al*., 2016; *Le Brocq et al*., 2011], although current model reconstructions for the pattern and timing of post-LGM retreat differ [*Briggs et al*., 2014; *Golledge et al*., 2014; *Gomez et al*., 2013; *Maris et al*., 2014; *Whitehouse et al*., 2012a] and the pattern of present-day uplift rates across the region is the subject of ongoing debate [*Bradley et al*., 2015; *Wolstencroft et al*., 2015]. Various modeling, geophysical, and field-based studies have hypothesized that the ice streams flowing into the Weddell Sea embayment have altered their course since the LGM [*Bingham et al*., 2015; *Glasser et al*., 2015; *Golledge et al*., 2012; *Hein et al*., 2016; *Siegert et al*., 2013; *Whitehouse et al*., 2012a; *Winter et al*., 2015] and that the grounding line may even have retreated behind its present position during the Holocene [*Bradley et al*., 2015; *Siegert et al*., 2013].

In this study we are concerned with the past ice dynamics of the eastern Weddell Sea, in particular, ice flow along the Filchner Trough (sometimes called "Thiel Trough") (Figure 1). Previous studies have focused on the marine record of ice sheet expansion along this trough and onto the outer continental shelf, where there is evidence for deformation of the bed by streaming ice, although this is not well dated [*Hillenbrand et al*., 2014; *Larter et al*., 2012]. However, using evidence from the Shackleton Range, which suggests that the LGM ice sheet was not significantly thicker than present in this region, *Hein et al*. [2011] hypothesized that grounded ice in the Filchner Trough did not advance beyond the outlet of the Recovery and Slessor Glaciers during the LGM. The LGM configuration of the Antarctic Ice Sheet in the eastern Weddell Sea therefore remains unresolved. Further upstream, evidence is beginning to emerge relating to the rate and magnitude of past ice thickness change in the Pensacola Mountains, which lie adjacent to the Foundation Ice Stream (FIS) (Figure 1) [*Balco et al*., 2016; *Bentley et al*., 2016]. We use these new data, which are briefly described in section 2, to motivate a study into the dynamics of the FIS and the adjacent ice shelf during the last glacial cycle. From here onward, "FIS" is used to describe both the grounded and floating components of the ice stream system.

While the future evolution of the FIS is not the focus of this study, we note that it has been hypothesized that a change in ocean circulation in response to future changes in sea ice coverage could result in an increase in the flux of warm circumpolar water into the Filchner Trough, thus increasing melt rates at the base of the Filchner Ice Shelf [*Hellmer et al*., 2012]. Investigations into the future stability of the Weddell Sea portion of the Antarctic Ice Sheet under such a scenario have concluded that this sector is likely to display a linear sea-level response to future ocean warming [*Mengel et al*., 2016] and, unlike the Institute and Möller Ice Streams, that the FIS is relatively stable in its current configuration [*Thoma et al*., 2015; *Wright et al*., 2014]. We seek to advance this discussion by exploring the long-term evolution of the FIS from the LGM toward its current configuration and to understand whether this evolution has included significant, or minimal, retreat.

The aims of our study are to determine the likely grounding line position and profile of the FIS during the LGM and to investigate whether the grounding line may have retreated behind its present position at some point during the Holocene. We do not seek to reconstruct precisely the time-transient evolution of the FIS throughout the last glacial cycle, a goal which is currently unfeasible due to the lack of constraints on temporal changes in accumulation and ocean forcing. Instead, we seek to investigate the sensitivity of FIS grounding line migration and along-flow ice surface profile to a range of potential controls. Specifically, we use a numerical flowline model, which is able to accurately simulate ice stream grounding line evolution [*Jamieson et al*., 2014; *Nick et al*., 2009; *Vieli and Payne*, 2005], to investigate the influence of changes in ice temperature, sea level, accumulation, ice shelf basal melt, and lateral drag on past ice dynamics. Model behavior is constrained by available geomorphological and dated field evidence. Where this is limited, sensitivity tests are undertaken to understand potential ice stream controls. We test the hypothesis that ice stream discharge routes have changed since the LGM, and we compare our results with the available field evidence in order to determine the most likely deglacial scenario.

We outline the existing field constraints relating to past ice thickness change in section 2. The model features and experiment design are described in section 3. Results for a suite of sensitivity studies are presented in section 4, and the implications of the model results are discussed in section 5.

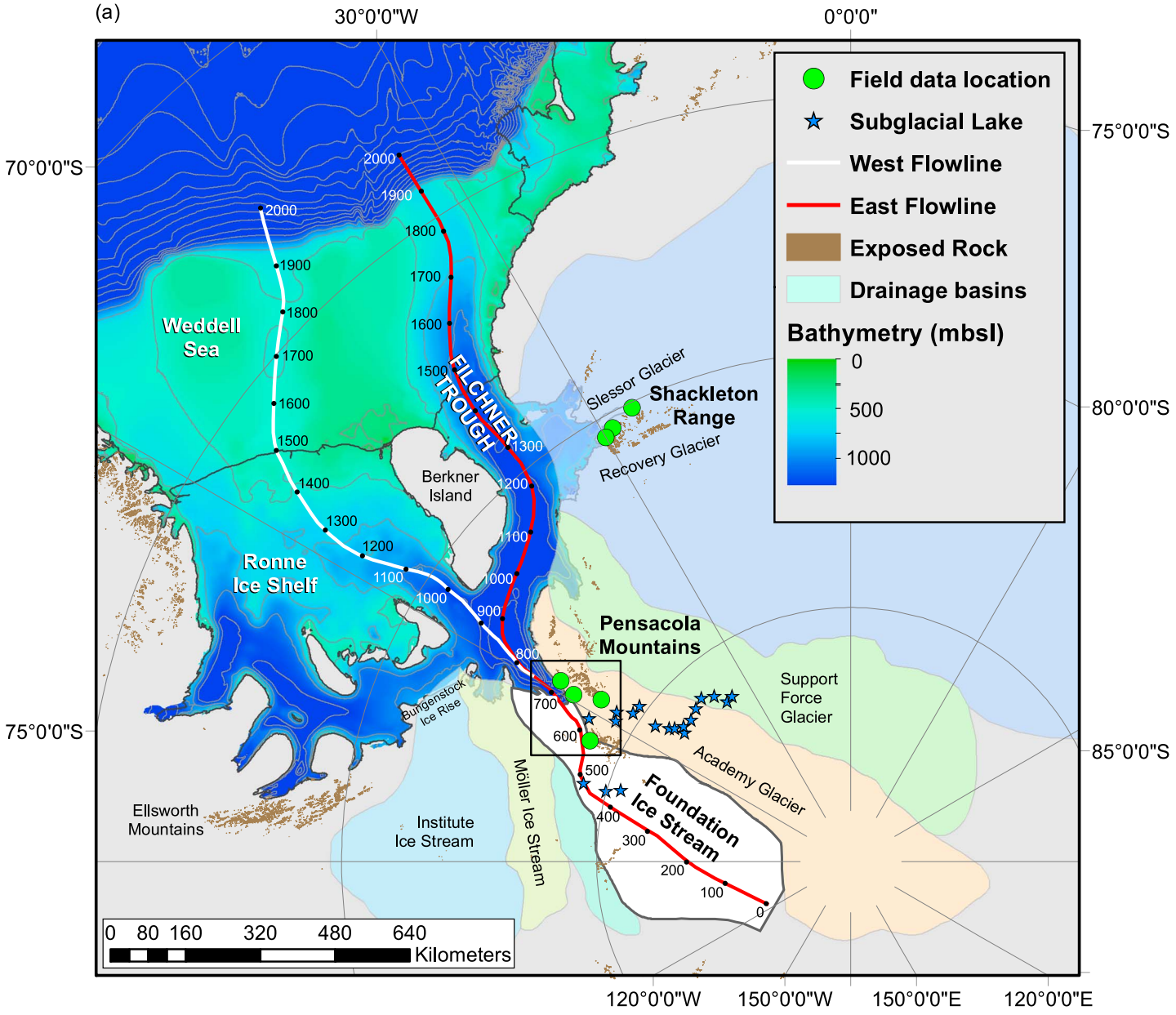

Figure 1. (a) Overview of study area. Bathymetry is shown for all areas offshore of the grounding line; contours are every 250 m; ice shelf extent is indicated by a thin black line. Grounded ice is shaded grey or in a color that delimits the drainage basins that are hypothesized to have discharged ice along the Filchner Trough during the Last Glacial Maximum. Net present-day accumulation within each drainage basin, taken from *Rignot et al.* [2008] is Institute Ice Stream 21.9 Gt/yr, Möller Ice Stream 7.4 Gt/yr; Foundation Ice Stream (including Academy Glacier and tributary to the west) 35 Gt/yr, Support Force Glacier 7 Gt/yr, Recovery Glacier 48.6 Gt/yr, and Slessor Glacier 30.6 Gt/yr. Distances along each flowline are given every 100 km. A black box indicates the region covered in Figure 1b. (b) Pensacola Mountains. Grounding line is from the Antarctic Digital Database; small colored circles indicate the elevation of the lower boundary of the ice sheet, as derived from Operation IceBridge data; inferred post-LGM ice thickness change is listed for each field site (green circle); shading is from the Landsat Image Mosaic of Antarctica; contours every 250 m.

2. Data

Geomorphological mapping and cosmogenic nuclide surface exposure dating have been used to study the former configuration of the expanded FIS during the local Last Glacial Maximum (LLGM) [*Balco et al.*, 2016; *Bentley et al.*, 2016].

At several sites along the margins of the FIS and its tributary, the Academy Glacier, there is dated geomorphic evidence of thicker ice at the LLGM (see Table 1 for references and Figure 1 for locations). For example, in the

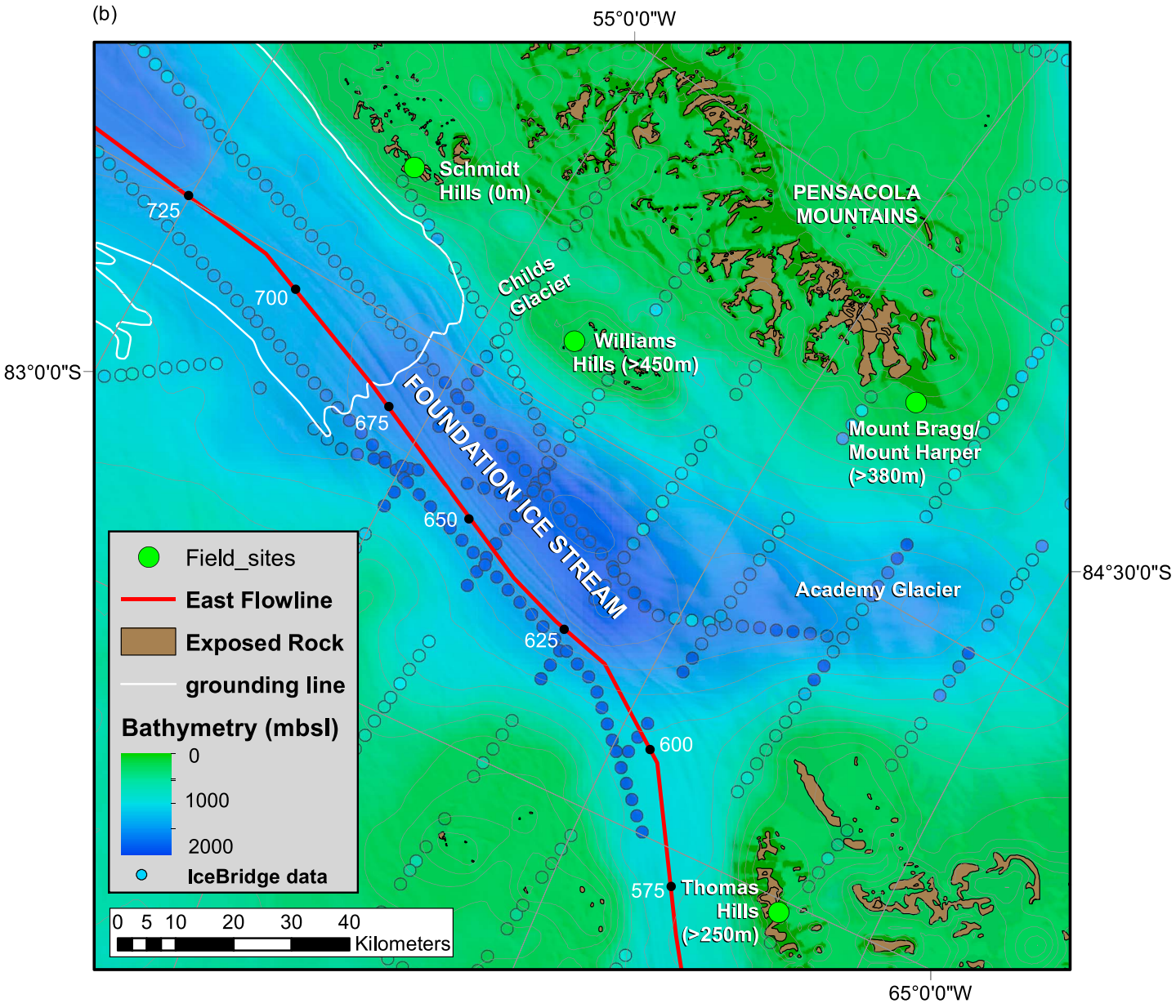

Figure 1. (continued)

Williams Hills ice was at least 450 m thicker, while further upstream in the Thomas Hills ice was at least 250 m thicker. These values are closely comparable to thickening further west in the Ellsworth Mountains, where ice was between 230 and 475 m thicker than present during the LLGM. Elsewhere, ice in the Shackleton Range was no thicker than present, which was shown by *Hein et al.* [2011] to limit any FIS thickening to <140 m. Ice core data demonstrate that Berkner Island was not overridden by inland ice during the LGM [*Mulvaney et al.*, 2007], and thus remained an independent flow center. This provides a further maximum constraint on ice thickness change in the region.

The timing of thinning can be determined from the exposure ages of progressively lower samples at each site. In Williams Hills the majority of deglacial thinning occurred in the interval 8.9 to 5.2 ka B.P.; at Mount Bragg and Mount Harper thinning occurred at 7.9 to 2.5 ka B.P. [*Bentley et al.*, 2016], and further upstream in the Thomas Hills there was a rapid interval of thinning at 7 ka B.P. [*Balco et al.*, 2016]. We note that these intervals of thinning are similar across the area and similar to the interval of major deglacial thinning at 6.5–3.5 ka B.P. in the southern Ellsworth Mountains [*Hein et al.*, 2016].

Table 1. Summary of Data Sets Recording Ice Thickness Change Since the LLGM Along Ice Streams Feeding the Southern Weddell Sea

Location, Ice Stream	Ice Thickness Change Since Local Last Glacial Maximum (m)[a]	Period of Maximum Thinning (ka B.P.)[b]	Source
Williams Hills, Foundation Ice Stream	≥450	8.9–5.2	*Bentley et al.* [2016]; *Balco et al.* [2016]
Mount Bragg and Mount Harper, Academy Glacier	≥380	7.9–2.5	*Bentley et al.* [2016]
Thomas Hills, Foundation Ice Stream	≥250	~7	*Balco et al.* [2016]; *Bentley et al.* [2016]
Shackleton Range, Slessor Glacier	~0 (implies ≤140 m change on FIS)	-	*Hein et al.* [2011]
S. Ellsworth Mountains, Institute Ice Stream	230–475	6.5–3.5	*Bentley et al.* [2010]; *Hein et al.* [2016]
Berkner Island, adjacent to Foundation Ice Stream	not overrun by inland ice	-	*Mulvaney et al.* [2007]

[a]All data except Berkner Island data are derived from geomorphological mapping and cosmogenic nuclide surface exposure dating.
[b]The interval when cosmogenic nuclide data suggest the most rapid thinning and the majority of deglacial change achieved; the precise onset and termination of thinning are not well constrained by the data.

3. Ice Stream Modeling

We use a 1-D numerical flowline model that was originally developed to track grounding line motion of an ice stream [*Vieli and Payne*, 2005]. The model is based on the shallow shelf approximation for ice flow and hence is a suitable tool for carrying out multiple sensitivity experiments of ice flow evolution from the Pensacola Mountains to the mouth of the Filchner Trough, a domain in which our modeled ice velocities are always >50 m/yr. The model has previously been adapted to include along-flow variations in ice stream width and an ice shelf component [*Jamieson et al.*, 2014, 2012; *Nick et al.*, 2009]. Here we further adapt this model by improving the ice shelf dynamics by modifying the treatment of large horizontal grounding line steps—as might occur when the front of an ice shelf, which is distant from the grounding line, touches down in shallow water. The geometry of the ice shelf in this improved model evolves with time, and temporal and spatial variations in ice shelf thickness and extent feed into lateral drag calculations. We use this updated model to investigate controls on the advance and retreat of the FIS, and the resulting change in ice thickness near the Pensacola Mountains and the Shackleton Range (Figure 1). We seek to answer two key questions: (i) what controlling factors is the advance and retreat of the FIS sensitive to? and (ii) what advance/retreat evolution is compatible with the evidence for ice thickness change recorded in the Pensacola Mountains and the Shackleton Range, and the past ice extent change inferred from the marine record? We investigate both of these questions in the context of the changes that could have occurred during the last glacial cycle, although we emphasize that our primary aim is to constrain the past configuration of the ice stream rather than reconstruct the precise timing of change.

The grounding line of the FIS currently lies approximately adjacent to the Schmidt Hills (Figure 1). Beyond the grounding line, floating ice from the FIS flows to the west of Berkner Island and is discharged at the calving front of the Ronne Ice Shelf, adjacent to the northern margin of Berkner Island. However, the bathymetry of the region (Figure 1) and previous 3-D modeling experiments [*Le Brocq et al.*, 2011; *Whitehouse et al.*, 2012a] suggest that grounded ice from the FIS has previously flowed east of Berkner Island along the Filchner Trough. This is supported by submarine geomorphological evidence for grounded ice near the mouth of the Filchner Trough [*Hillenbrand et al.*, 2014, 2012; *Larter et al.*, 2012]. We therefore investigate the dynamics of ice flow along paths both to the east and west of Berkner Island in our modeling experiments.

3.1. Model Setup

The 1-D flowline model of *Vieli and Payne* [2005] is adapted to investigate ice stream and ice shelf dynamics in the south-east Weddell Sea. This model was included in the recent Marine Ice Sheet Model Intercomparison Project [*Pattyn et al.*, 2012], where it was found to robustly simulate grounding line migration and be consistent with boundary layer theory [*Schoof*, 2007]. Although 3-D models that can robustly simulate grounding line motion are now emerging, we prefer to use a reduced flowline modeling approach for two reasons. First, a flowline model can be run at high spatial resolution and its fast run time (relative to 3-D models) makes it possible to explore ice stream behavior in response to a large suite of forcing parameters, over multimillennial time scales. Second, input data on boundary conditions (bed topography, basal sliding, etc.) are very limited and poorly constrained for 3-D simulations. This would give rise to substantial uncertainty when attempting to model a complex 3-D system. Since our aim is to carry out a series of sensitivity experiments

that explore the first-order relationship between grounding line position and the evolution of along-flow ice thickness we believe that the optimum tool for such an exercise is a flowline model.

The model domain consists of 2400 equal-sized cells that cover the region from the ice divide to a location ~80 km offshore of the continental shelf, i.e., both the grounded and floating portions of the FIS are represented within a single domain. The position of the ice divide is held fixed throughout all experiments, the uniform cell size at the start of each model run is 1 km, and the use of an evolving grid means that the cell size at the end of each experiment is between 0.9 and 1.2 km depending on the change in grounding line position. This evolving grid tracks the migration of the grounding line as follows: at the end of each time step a flotation criterion [*Vieli and Payne*, 2005] is used to identify the grid cell that contains the grounding line, and linear interpolation of ice thickness within this cell is used to determine the precise position of the grounding line. The grid is then re-meshed by specifying that (i) the new grounding line must be defined by a grid point (the nearest grid point is shifted to this new grounding line position), (ii) the number of cells upstream of this grid point is unchanged, (iii) the position of the ice divide is unchanged, and (iv) for a given time step the size of every cell is equal. This approach of re-meshing the grid by moving the nearest grid point to the position of the new grounding line (rather than, e.g., tracking the grounding line using the same grid point for the whole experiment) minimizes the change to the cell size across each time step (see Figure S1 in the supporting information). Our method can also deal with scenarios in which the grounding line migrates a significant distance (e.g., tens of kilometers) in a single time step, or an ice rise is created or destroyed (see section 3.1.4). The default time step used within the model is 0.005 years (~2 days), but this is reduced if ice velocities exceed ~20 km/yr.

The model is isothermal and includes a number of parameters that can be varied over time (see section 3.2). Inputs to the model include information relating to bed elevation and ice stream width along each flowline, basal sliding conditions in the grounded portion of the ice stream, melt rates at the base of the floating ice shelf, ice temperature, accumulation rates, and tributary ice fluxes. Profiles of ice thickness and velocity along a central flowline are required to initialize each experiment, and the evolution of ice thickness, ice flow, and stress is determined by considering the stress balance:

$$2\frac{\partial}{\partial x}(H\tau_{xx}) - \tau_b - \tau_{\text{lat}} = -\tau_d \tag{1}$$

In equation (1) H is ice thickness (m), and the driving stress, τ_d, is balanced by basal stress, τ_b; lateral shear stress, τ_{lat}; and the longitudinal stress gradient in the direction of flow, $\partial\tau_{xx}/\partial x$. Lateral shear stress is determined by assuming zero flow at the ice stream margins [*Van der Veen and Whillans*, 1996], and we use a Weertman-type nonlinear sliding relation [*Weertman*, 1957] to calculate basal stress where the ice is grounded:

$$\tau_b = \beta|u|^{m-1}u \tag{2}$$

In equation (2), u is ice velocity, $m = 1/3$, and β is assumed to be linearly proportional to the effective pressure at the bed:

$$\beta = \beta_{in}(\rho_i g H + \min[\rho_w g z, 0]) \tag{3}$$

In equation (3), z is bed elevation (m), defined to be negative below sea level; ρ_i and ρ_w are the density of ice (910 kg m^{-3}) and water (1028 kg m^{-3}), respectively; g is gravitational acceleration (9.81 m s^{-2}); and β_{in} is a user-defined, spatially variable basal traction parameter which is used to specify basal friction in different geological settings (see below). A threshold is set within the flowline model to ensure that β is positive at all points up to and including the grounding line; β is set to zero offshore of the grounding line.

Assuming an ice stream of half-width W and ice thickness H (ice thickness is assumed to be uniform across the width of the ice stream), the stress balance in equation (1) yields an expression for depth- and width-averaged ice velocity, u:

$$2\frac{\partial}{\partial x}\left(Hv\frac{\partial u}{\partial x}\right) - \beta|u|^{m-1}u - \frac{H}{W}\left(\frac{5}{2AW f_{\text{lat}}}\right)^{\frac{1}{n}}|u|^{\frac{1}{n}-1}u = \rho_i g H\frac{\partial S}{\partial x} \tag{4}$$

In equation (4), v is effective viscosity, $\partial u/\partial x$ is a strain rate, A is the temperature-dependent flow rate factor in Glen's flow law [*Glen*, 1955], S is the ice surface, and n (=3) is the exponent in Glen's flow law, which states the

constitutive relationship between stress and strain rate when considering the viscous flow of ice. In all cases we assume $m = 1/n$. A buttressing factor, f_{lat}, controls the strength of lateral drag exerted at the margins of the ice stream. Within the flowline model f_{lat} can be altered for either the grounded or floating portions of the ice stream (or both); for all experiments considered here f_{lat} is only altered along the floating portion of the ice stream. $f_{lat} = 1$ is the case where the full effect of lateral drag is felt, while values of $f_{lat} > 1$ nonlinearly reduce the magnitude of the buttressing that is applied to the margins of the ice stream. Situations in which values of $f_{lat} > 1$ might apply are discussed below.

Equation (4) is solved by iteratively determining the effective viscosity, which is given by

$$v = A^{-1/n}\left|\frac{\partial u}{\partial x}\right|^{(1-n)/n} \tag{5}$$

Lastly, ice surface evolution along the central flowline of an ice stream is determined by solving the continuity equation, taking into account along-flow variations in ice stream width, accumulation (a), and basal melt (b):

$$\frac{\partial H}{\partial t} = (a - b) - \frac{1}{W}\frac{\partial (uHW)}{\partial x} \tag{6}$$

Details of the specific model setup used to investigate controls on the dynamics of the FIS are given in the following sections.

3.1.1. Geometry

BEDMAP2 [*Fretwell et al*., 2013] is used to define the topographic profile along the two flowlines. The data that constrain BEDMAP2 in this region come from radar and seismic soundings [*Fretwell et al*., 2013; *Timmermann et al*., 2010, and references therein]. At each grid point, BEDMAP2 values are smoothed over a 30 km radius so that the bed profile of each flowline is representative of topography across the wider ice stream. BEDMAP2 includes a prominent bedrock high in the region of the present-day grounding line (Figure 1), which will influence local grounding line dynamics. We note that this feature is poorly resolved by the data sets used to construct BEDMAP2 [*Fretwell et al*., 2013], and therefore use radar data from Operation IceBridge [*Gogineni*, 2012] to supplement our bed geometry data set. These data provide information relating to the elevation of the upper and lower surfaces of ice (floating or grounded) in the region of the present-day grounding line. In particular, across the bedrock high these data imply that the base of the ice lies below the height of the bed according to BEDMAP2 (Figure 1), which cannot be the case. It is not possible to determine the actual depth of the bed because the radar data only provide information on the elevation of the base of the ice, as derived from subtracting ice thickness from absolute ice surface elevation. Therefore, for the short region upstream of the grounding line where the data are in conflict (between 685 and 725 km from the ice divide; see Figure 1) we assume that the bed lies at approximately the same depth as the base of the ice and the topography profile is edited accordingly.

Model parameters, such as bed depth, are interpolated onto the evolving grid by using splines. The width of the ice stream controls the lateral stress that is exerted along the flowline; width is estimated by using the Landsat Image Mosaic of Antarctica (http://lima.usgs.gov) to identify current shear margins at the edge of the grounded portion of the FIS and BEDMAP2 to delineate the edge of submarine troughs in regions where ice is not currently grounded.

3.1.2. Basal Conditions

A user-defined basal traction parameter, β_{in}, is defined for each point along a flowline such that larger values of β_{in} result in higher shear stresses at the bed (equations (2) and (3)). Within the flowline model this basal traction parameter is multiplied by the ice overburden pressure with the result that basal shear stress (equation (2)) evolves as the ice stream evolves, increasing as the ice gets thicker or faster, or as the ice surface gets steeper (noting that ice velocity depends on surface slope via equation (4)).

Where the bed lies below sea level a low value of β_{in} is assigned, in agreement with earlier modeling approaches [*Jamieson et al*., 2014; *Le Brocq et al*., 2011; *Whitehouse et al*., 2012a], which assumed that these regions contain soft deformable marine sediments. A low basal traction parameter is also defined where the ice stream passes over known subglacial lakes (Figure 1) [*Smith et al*., 2009]. During initial sensitivity experiments the value for β_{in} in each of the three domains (above/below sea level and subglacial lakes) was optimized via manual tuning to the present-day ice surface. These β_{in} values, which yield basal shear

stresses of 20–40 kPa in the region of the current grounding line in agreement with *Joughin et al*. [2006], were used in all subsequent experiments.

3.1.3. Mass Balance and Ice Shelf Processes

Mass input to the ice stream is via snowfall. Within the model, mass input at each point along the flowline is determined by integrating spatially variable accumulation rates over the width of the region drained by the FIS. Where a tributary ice stream joins the FIS, mass input from this ice stream is included in the surface mass budget, with the input being distributed over the length of the flowline that is adjacent to the tributary glacier (Figure 1). Present-day accumulation rates are taken from *Arthern et al*. [2006], and sensitivity experiments used a scaled version of this spatial pattern to reflect the change in accumulation between glacial and interglacial periods (see section 3.2).

Mass is lost from the ice stream system via basal melting of the ice shelf and iceberg production at the calving front. Surface melting is assumed to be negligible due to the persistence of subzero air temperatures throughout the last glacial cycle. Ice shelf basal melt rates are assumed to depend on the depth to the base of the ice shelf. Rates are constructed (see below) so that they vary linearly between user-defined minimum and maximum values for depths between 0 and 1500 m, respectively. The minimum melt rate is never actually applied because a minimum ice shelf thickness of 200 m (a realistic value for an ice stream of this size) is enforced to prevent runaway thinning. If the ice shelf base lies below 1500 m depth the maximum basal melt rate is applied. During sensitivity experiments the minimum melt rate is held fixed, while the maximum melt rate is altered to reflect the influx of ocean water of different temperatures.

The present-day relationship between basal melt rate and depth is determined from satellite-derived observations of ice velocity, which are combined with observations of ice thickness and accumulation rates to determine basal melt rates in the region immediately offshore of the FIS grounding line, assuming steady state [*Makinson et al*., 2011]. The maximum basal melt rates used in the present-day experiments are lower than the basal melt rates inferred at the current grounding line of the FIS (~3.5 m/yr [*Makinson et al*., 2011]), where the base of the ice shelf lies at a depth of ~1400 m. However, these localized high basal melt rates are hypothesized to be due to dynamic processes associated with the upwelling of buoyant subglacial meltwater that is discharged across the grounding line and the entrainment of warmer water from the adjacent ocean cavity into this rising plume [*Jenkins*, 1991; *Le Brocq et al*., 2013]. The approximation that basal melt rates increase linearly with depth therefore may break down adjacent to the grounding line. Accounting for such dynamic processes is beyond the scope of our model: we did investigate the effect of using a steeper gradient of basal melting below depths of 1500 m but found that this had a negligible effect on our model results. Our decision to use a constant melt rate below 1500 m depth is justified by the close agreement between observed and modeled present-day ice shelf thickness along the majority of the flowline profiles [*Makinson et al*., 2011], although we note that it is not possible to determine how accurately our model setup is able to reproduce the basal melt profile during glacial conditions.

3.1.4. Ice Shelf Dynamics

In our version of the flowline model, the ice shelf is assumed to be made up of a specific number of cells, of minimum thickness 200 m, which expand or contract as the grid is re-meshed in response to grounding line migration. This assumption acts as a proxy for a calving law; it prevents the ice shelf from growing or shrinking too rapidly, but it does allow the ice shelf to evolve as the grounding line evolves. During grounding line migration, the number of cells that make up the ice shelf is recalculated, ensuring that the frontal position of the ice shelf is preserved as closely as the gridding scheme allows and the change in cell size is minimized (see Figures S2 and S3). This update to earlier versions of the flowline model allows us to test FIS sensitivity to scenarios in which the ice shelf grounds at a remote location, forming an ice rise. In such a case, the model is able to deal with the presence of multiple grounding lines and the formation of an ocean cavity upstream of the most offshore grounding line position (see Movie S1 in the supporting information).

In addition to the careful treatment of ice shelf evolution during grounding line migration, this version of the flowline model also removes portions of the ice shelf that extend across regions where the bed is deeper than −3000 m. Depths of this magnitude are only found offshore of the continental shelf, where the Weddell Sea embayment is laterally unconstrained, and therefore, it is unlikely that an ice shelf could be sustained due to the large tensile stresses that would be applied at the calving front [*Pollard and DeConto*, 2012].

Table 2. Parameter Values Used to Define Glacial and Interglacial Conditions in the Numerical Experiments

Parameter[a]	Interglacial Conditions	Glacial Conditions
Ice temperature (°C)	−20	−30
Maximum ice shelf basal melt rate (m/yr)	1.2/1.5[b]	0.5
Sea level (m, relative to present)	0	−100
Accumulation rates (%, relative to present)	100	50

[a]All changes are applied linearly over a 2000 year period.
[b]1.2 m/yr is used for the West flowline; 1.5 m/yr is used for the East flowline.

Ice shelves play an important role in modulating ice sheet dynamics, and episodes of reduced ice shelf buttressing will have a strong impact on ice stream flow and grounding line migration [*Dupont and Alley*, 2005]. Within the flowline model ice shelf buttressing can be reduced by setting $f_{lat} > 1$ (equation (4)) in regions where ice is floating. This decreases the magnitude of lateral drag applied at the margins of the ice shelf and mimics the development of a weak marginal shear zone or, in a more extreme case, the total collapse of the floating ice shelf. In both situations, the resistive force applied at the grounding line would be decreased, thus altering the stress regime throughout the grounded portion of the ice stream. Within the flowline model a gradual return to the case $f_{lat} = 1$ is used to represent the scenario in which full lateral drag is re-established following the re-growth of a strong ice shelf.

3.2. Experiment Design

Experiments are designed to (i) reproduce present-day ice stream geometry and dynamics, (ii) investigate ice stream response to the onset of glacial conditions, and (iii) investigate ice stream response to the onset of interglacial conditions. In particular, we quantify the changes in along-flow ice thickness, grounding line position, and ice shelf geometry that occur following the onset of glacial/interglacial conditions. Experiments are carried out for flowlines running both west and east of Berkner Island.

In order to assess the performance of the present-day experiments in reproducing present-day conditions, model output is compared with observations of ice velocity [*Rignot et al*., 2011], ice surface elevation [*Fretwell et al*., 2013], and ice shelf thickness. Ice shelf thickness is derived from the surface elevation observations assuming an ice density of 910 kg/m^3 and an ocean density of 1028 kg/m^3. However, we note that true ice shelf thicknesses may vary by 5–10% from our calculated values due to variations in ice and ocean density [*Cuffey and Paterson*, 2010].

In order to assess how well the advance and retreat experiments reproduce the behavior recorded by the field data (see section 2), we assume that ice thickness change is uniform across the whole width of the ice stream, and hence that modeled thickness change on the flowline reflects thickness change at the adjacent field sites. Limitations of this approach are discussed in section 5. Two other points should be noted. (i) To account for any errors in our present-day reconstructions, the *change* in ice thickness during advance and retreat is considered, rather than absolute ice thickness adjacent to each field site. (ii) By comparing the field data with modeled ice thickness change rather than modeled ice surface elevation change we circumvent the issue of whether there was any change in the absolute elevation of the field site.

Parameters that may be varied in the present-day experiments are the uniform ice temperature and ice shelf basal melt rates. Additional parameters that may be varied in the advance and retreat experiments are sea level, accumulation rates, and (for the retreat experiments only) the magnitude of lateral drag along floating portions of the ice stream. A brief description of how each parameter is varied is given below; the actual values used in each experiment can be found in Tables 2 and 3.

3.2.1. Ice Temperature

Since the model is isothermal, ice temperature changes are applied uniformly along the length of the ice stream, and at all depths. Guided by glacial-interglacial temperature variations determined from the analysis of nearby ice cores [*Huybrechts et al*., 2007], ice temperatures are varied by 10°C to represent the transition between glacial and interglacial conditions.

3.2.2. Ice Shelf Basal Melt Rates

The maximum basal melt rate is varied between experiments, and this alters the rate at which basal melting increases with depth. Lower basal melt rates are assumed to have persisted during glacial periods due to the

Journal of Geophysical Research: Earth Surface

10.1002/2016JF004121

Table 3. Details of All Numerical Experiments Carried Out

Expt ID	Flowline (W/E)[a]	Ice Temp. (°C)[b]	Max. Basal Melt Rate (m/yr)[b]	Sea Level (m)[b]	Accumulation Rate (% of Modern)[b]	Reduction in Lateral Drag (%; 1 s.f.)[c]	Initial Conditions	Notes: Including summary of whether ice steam grounding line advanced or retreated in each experiment[d]
Present-Day Experiments								
P1	W	−20	1.2	0	100	-	observed	Good agreement with observed FIS geometry
P2	E	−20	1.5	0	100	-	observed	Good agreement with observed FIS geometry
Interglacial to Glacial ("Advance") Experiments								
A1	W	−20/−30	1.2/0.5	0/−100	100/50	-	observed	Control: advance to continental shelf (CS)
A2	E	−20/−30	1.5/0.5	0/−100	100/50	-	observed	Control: advance to Berkner Island (BI)
A3	E	−20/−30	1.5	0	100	-	observed	Just vary ice temperature: no advance
A4	E	−20	1.5/0.5	0	100	-	observed	Just vary basal melt: advance to BI
A5	E	−20	1.5	0/−100	100	-	observed	Just vary sea level: no advance
A6	E	−20	1.5	0	100/50	-	observed	Just vary accumulation: slight (~50 km) retreat
A7	E	−20/−30	1.5	0/−100	100/50	-	observed	Vary all except basal melt: no advance
A8	E	−20/−30	1.5/0.75	0/−100	100/50	-	observed	Greater basal melt: no advance
A9	E	−20/−30	1.5/0.5	0/−100	100/50	-	observed	Include extra flux: advance to CS
[e]*Glacial to Interglacial ("Retreat") Experiments*								
R1	W	−30/−20	0.5/1.2	−100/0	50/100	50	A1	Moderate reduction in buttressing: no retreat
R2	W	−30/−20	0.5/1.2	−100/0	50/100	80	A1	Strong reduction in buttressing: no retreat
R3	E	−30/−20	0.5/1.5	−100/0	50/100	50	A2	Moderate reduction in buttressing: retreat to present-day grounding line position
R4	E	−30/−20	0.5/1.5	−100/0	50/100	80	A2	Strong reduction in buttressing: retreat to ~100 km behind present position, then re-advance to present
R5	E	−30/−20	0.5/1.5	−100/0	50/100	50	A9	Moderate reduction in buttressing: ~40 km retreat
R6	E	−30/−20	0.5/1.5	−100/0	50/100	80	A9	Strong reduction in buttressing: retreat to present-day grounding line position
R7	E	−30/−20	0.5/1.5	−100/0	50/100	-	A2	Vary all parameters except buttressing: partial (~150 km) retreat
R8	E	−30	0.5	−100	50	50	A2	Only decrease buttressing: temporary, partial (~300 km) retreat during reduced buttressing
R9	E	−30/−20	0.5	−100	50	-	A2	Vary ice temp., do not reduce buttressing: partial (~300 km) retreat
R10	E	−30	0.5/1.5	−100	50	-	A2	Vary basal melt, do not reduce buttressing: no retreat
R11	E	−30	0.5	−100/0	50	-	A2	Vary sea level, do not reduce buttressing: no retreat
R12	E	−30	0.5	−100	50/100	-	A2	Vary accumulation, do not reduce buttressing: advance to CS
R13	E	−30/−20	0.5	−100	50	50	A2	Vary ice temperature, reduce buttressing: retreat
R14	E	−30	0.5/1.5	−100	50	50	A2	Vary basal melt, reduce buttressing: temporary, partial (~350 km) retreat during reduced buttressing
R15	E	−30	0.5	−100/0	50	50	A2	Vary sea level, reduce buttressing: temporary, partial (~450 km) retreat during reduced buttressing
R16	E	−30	0.5	−100	50/100	50	A2	Vary accumulation, reduce buttressing: advance to CS

[a] W = West, E = East flowline.
[b] "*x*/*y*" denotes conditions at the start and end of the experiment; if only one value is given that parameter is held constant throughout the experiment.
[c] Reduced lateral drag is only applied for 1000 years at the onset of interglacial conditions in the retreat experiments.
[d] In the "control" experiments all parameters are varied.
[e] Retreat experiments are initialized by using output from advance experiments.

circulation of colder water beneath the Filchner and Ronne ice shelves, but a lack of proxy data relating to paleo-ocean temperatures in this region means that our sensitivity experiments are poorly constrained.

3.2.3. Sea Level

Changes to the mass and extent of the Antarctic Ice Sheet during the last glacial cycle will have deformed the solid Earth and altered the shape of the gravitational field such that water depth changes at the grounding line will not have tracked global mean sea-level change [*Farrell and Clark*, 1976]. It is beyond the scope of this study to self-consistently model the response of the solid Earth and the geoid to regional ice mass change. Instead, we use output derived from a glacial isostatic adjustment (GIA) model [*Whitehouse et al*., 2012b] to estimate water depth changes near the edge of the continental shelf during the last glacial cycle, i.e., in potential LGM grounding line locations. The net change in sea level near the mouth of the Filchner Trough was found to be ~100 m (fall and then rise) during the last glacial cycle, which is ~20 m less than the net eustatic change. The relatively small departure from eustasy is due to the fact that the ice sheet reconstruction used in the GIA model assumes relatively thin ice near the edge of the continental shelf during the LGM [*Whitehouse et al*., 2012a].

For the purposes of this study a glacial-interglacial sea-level change of 100 m was prescribed in the sensitivity experiments by applying a uniform shift to the topography values. However, we note that the departure from eustasy would have varied along the length of the flowline and evolved with time according to the change in ice loading, making it impossible to prescribe in advance the precise water depth at the grounding line for different scenarios. Indeed, *Gomez et al*. [2010] demonstrated that GIA feedbacks cause water depth changes at the grounding line to be of the opposite sign to the eustatic change. This counterintuitive result has a stabilizing effect on ice dynamics; such feedbacks should be included in future studies of grounding line dynamics.

3.2.4. Accumulation Rates

Present-day accumulation rates are halved during the ice advance experiments and then increased back to their original values during ice retreat experiments, reflecting the lower accumulation rates recorded during glacial periods in the Antarctic interior [*Huybrechts et al*., 2007; *Siegert*, 2003]. Ice flux from tributaries of the FIS are altered accordingly, and we also include one experiment in which the Institute and Möller Ice Streams are assumed to have been tributaries of the FIS during the last glacial period, as suggested by *Siegert et al*. [2013].

3.2.5. Ice Shelf Lateral Drag

Buttressing by a floating ice shelf can be lost due to a number of factors, including a reduction in the length or thickness of the ice shelf, mechanical weakening due to crevasse growth, or the development of a shear zone at the margin of the ice shelf. The flowline model is not capable of representing all these individual processes, and instead, we test the importance of a reduction in ice shelf buttressing by varying the lateral drag parameter f_{lat} (equation (4)) in regions where ice is floating. We consider two scenarios: in the first case lateral drag is gradually reduced by ~50% during the first 500 years of the onset of interglacial conditions ($f_{\mathrm{lat}} = 10$). In the second case lateral drag is gradually reduced by ~80% over the same period ($f_{\mathrm{lat}} = 100$). In both cases full lateral drag is gradually reinstated along the length of the ice shelf during the subsequent 500 years by allowing f_{lat} to return to its original value ($f_{\mathrm{lat}} = 1$).

3.2.6. Experiment Parameters and Boundary Conditions

For the present-day experiments the model is run for 2000 years; for all other experiments the model is run for 9000 years. These run-times are long enough that the system approximately reaches a new equilibrium state by the end of each experiment. Present-day and interglacial-to-glacial experiments are initialized by using estimates of present-day ice velocity and thickness [*Fretwell et al*., 2013; *Rignot et al*., 2011], while output from the final time step of the interglacial-to-glacial experiments is used to initialize the glacial-to-interglacial experiments.

Since boundary conditions such as basal topography are imperfectly known, the interglacial-to-glacial experiments are spun-up for a period of 1000 years prior to varying the forcing parameters, to ensure that the modeled velocity, ice thickness, and grounding line position are internally consistent. Changes to these values were found to be negligible by the end of the spin-up period, and the same spin-up period is also used for the interglacial-to-glacial experiments for consistency.

Forcing parameters are then varied from their initial values to their final values over 2000 years, and these final values are then maintained for a further 6000 years. We note that the processes represented by the forcing parameters will operate on different characteristic time scales. However, since we wish to vary all

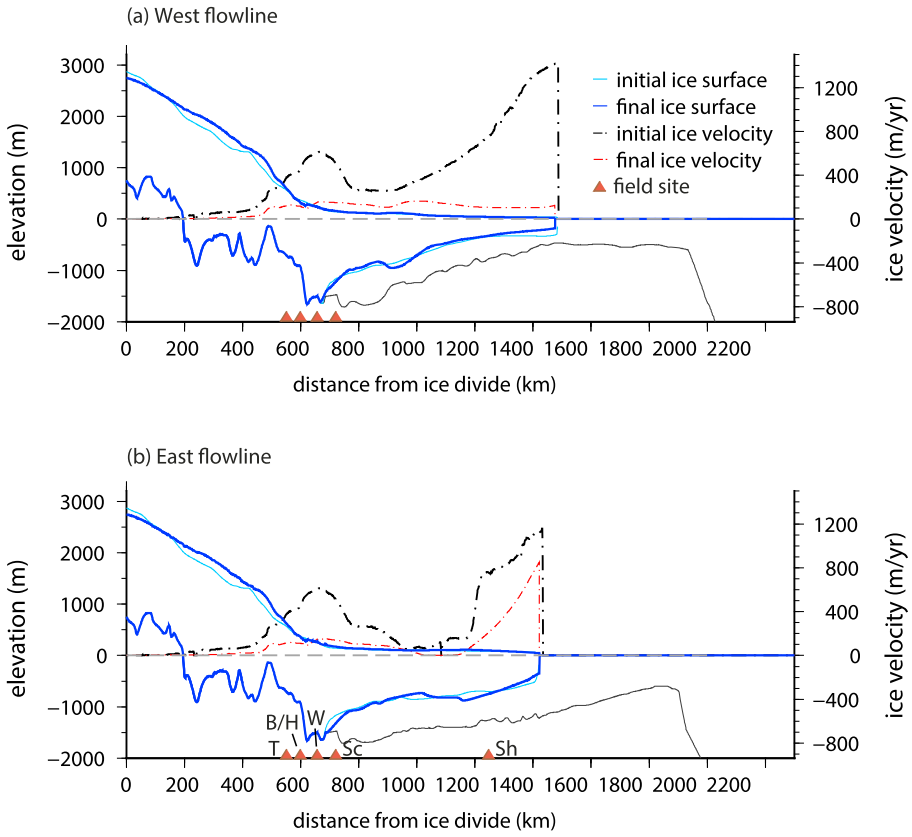

Figure 2. Observed (pale blue line) and modeled (dark blue line) present-day ice stream geometry for grounded and floating portions of the (a) West and (b) East flowlines. Observed (black dash-dotted line) and modeled (red dash-dotted line) ice velocities are also shown. The locations of field sites along each flowline are indicated on the *x* axis; site names are given in Figure 2b: T = Thomas Hills, B/H = Mount Bragg/Mount Harper, W = Williams Hills, Sc = Schmidt Hills, Sh = Shackleton Range. Note that the West flowline does not pass the Shackleton Range (see Figure 1).

parameters over the same period, 2000 years is chosen as an intermediate time scale for changes in ice temperature, accumulation, sea level, and ocean temperature. Model output is recorded every 20 years, and modeled ice thickness changes adjacent to the field sites, summarized in section 2, are extracted and compared with ice thickness changes inferred from the field data.

Control experiments are carried out for both flowlines with the aim of investigating the sensitivity of the FIS to the onset of glacial or interglacial conditions. Initial and final parameter values for these control experiments are given in Table 2; parameters are varied from their interglacial values to glacial values when investigating the response to the onset of glacial conditions, and vice versa when investigating the response to the onset of interglacial conditions. A number of additional sensitivity experiments are carried out, the details of which can be found in Table 3.

4. Results

4.1. Present-Day Experiments (Experiments P1 and P2)

Our reconstructions for the present-day ice stream-ice shelf geometry are produced by using an ice temperature of −20°C, and a maximum basal melt rate of 1.2 m/yr for the West flowline and 1.5 m/yr for the East flowline. During each model run the grounding line migrates to reach a new stable position that lies within 25 km of the initial position, and overall, the model results are in close agreement with observations (Figure 2). Observed velocities for the West flowline are not reproduced because ice flux across the Ronne Ice Shelf is enhanced by ice stream contributions from the south-west Weddell Sea, not modeled here. The maximum and mean absolute misfit between modeled and observed ice surface elevations at locations adjacent to our field sites are 39 m and 28.8 m for the West flowline and 18 m and 9.2 m for the East flowline, respectively

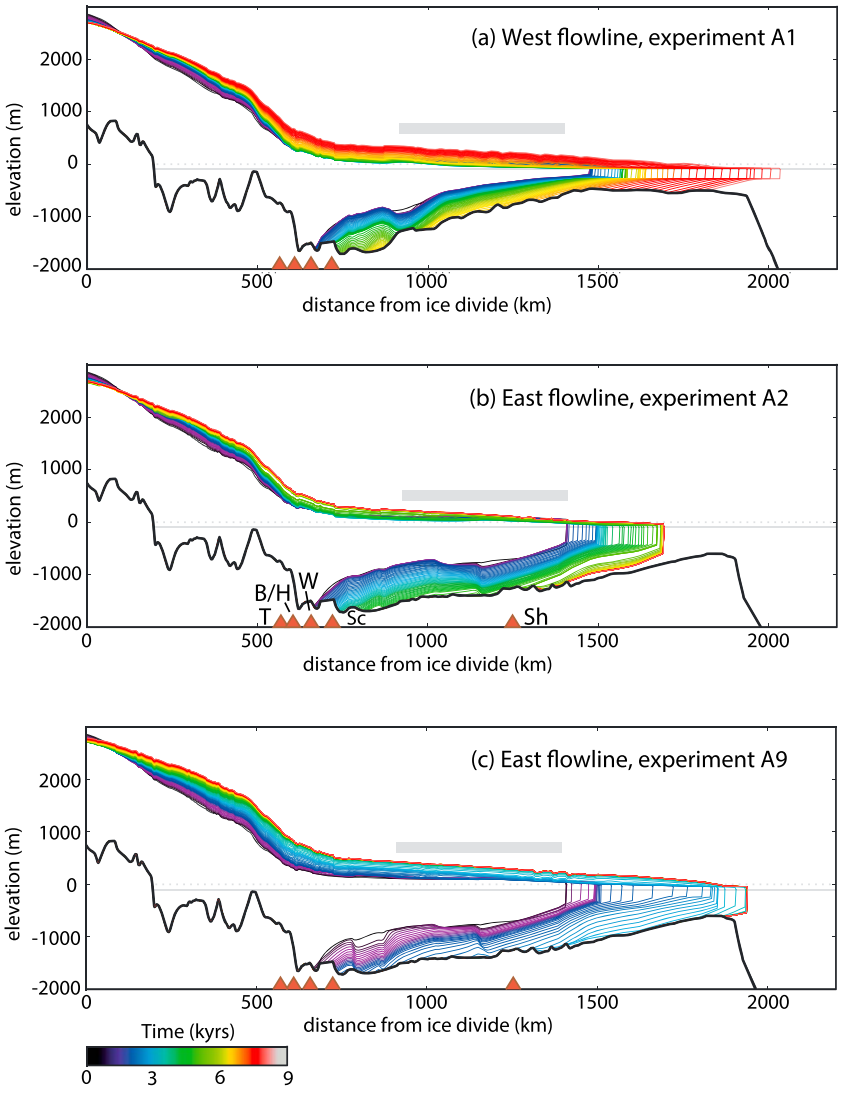

Figure 3. (a) Modeled evolution of ice thickness along the West flowline in response to the onset of glacial conditions (experiment A1, Table 3). Model output is shown every 100 years according to the color scale. The horizontal dotted and solid grey lines are the initial and final sea level, respectively, and the approximate extent of Berkner Island is indicated by the horizontal grey bar. Field site locations are indicated on the *x* axis by brown triangles; site names are given in Figure 3b as for Figure 2. (b) As for Figure 3a but for the East flowline (experiment A2, Table 3). (c) As for Figure 3b but for the experiment in which the Institute and Möller ice streams contribute to the ice flux along the Filchner Trough (experiment A9, Table 3).

(Figure 2 and Table S1 in the supporting information). We note that these misfits are a few tens of meters smaller than the misfits that were achieved prior to editing the bathymetry in the region of the present-day grounding line (edits were carried out to satisfy IceBridge radar data; see section 3.1), and they are up to hundreds of meters smaller than the misfits achieved in previous studies [*Golledge et al.*, 2012; *Whitehouse et al.*, 2012a].

4.2. Response to the Onset of Glacial Conditions

The parameters used in the control experiments, which are designed to replicate the response of the FIS to the onset of glacial conditions, are given in Table 2.

4.2.1. West Flowline Control Experiment (Experiment A1)

The evolution of ice thickness along a flowline that runs west of Berkner Island is shown in Figure 3a (see also Movie S1). Ice from the FIS currently follows this trajectory, and therefore we postulate that the first few thousand years of this model run likely reflect the evolution of the FIS during the initial stages of any glacial period where the initial (interglacial) grounding line was located near to the current position of the grounding line.

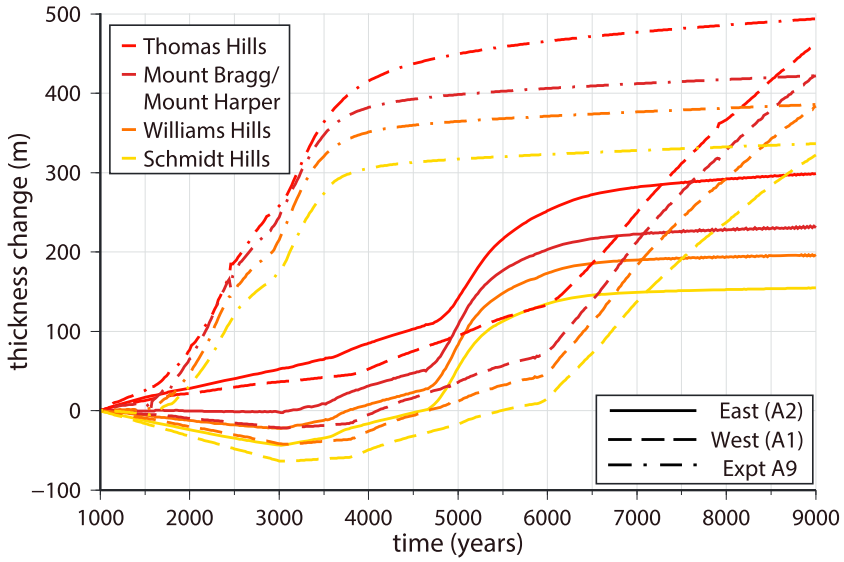

Figure 4. Modeled ice thickness change at field sites in the Pensacola Mountains, in response to the onset of glacial conditions. Results for the West (experiment A1, Table 3) and East (experiment A2, Table 3) flowline are shown by dashed and solid lines, respectively. Results for the case where ice advances to the continental shelf break along the East flowline (experiment A9, Table 3) are shown by dash-dotted lines.

Due to the deep bathymetry north of the present-day grounding line the model predicts an ~200 km jump in the position of the most offshore location of grounded ice ~3000 years after the onset of glacial conditions, rather than gradual grounding line advance. This jump occurs during a single time step following a period of ice shelf thickening west of Berkner Island. As the ice shelf grounds on the shallow bed adjacent to the southern margin of Berkner Island, the increase in basal stress alters the dynamics of the region immediately upstream of the newly grounded region and one of two situations is likely to occur. (i) The decrease in ice velocity upstream of the newly grounded region leads to ice thickening, and eventual grounding along the whole flowline, as depicted in Figure 3a. (ii) Alternatively, floating ice south of the newly grounded region is diverted east of Berkner Island, where the only resistance to flow is provided by lateral drag along the margins of the floating ice shelf (as long as the grounding lines of the Support Force, Recovery and Slessor glaciers have not advanced into the deep Filchner Trough). We do not have the capacity to model such "flow-switching" by using our 1-D model, but note that several recent modeling studies predict that ice from the FIS flows east of Berkner Island during full glacial conditions [*Golledge et al.*, 2012; *Golledge et al.*, 2013; *Le Brocq et al.*, 2011; *Whitehouse et al.*, 2012a]. This configuration has also been suggested based on the identification of glacial lineations and drumlinoid features within the Filchner Trough—features that are indicative of fast-flowing ice, and the identification of grounding zone wedges on the outer continental shelf [e.g., *Hillenbrand et al.*, 2014; *Larter et al.*, 2012; *Stolldorf et al.*, 2012]. We therefore adopt this second scenario as being the most likely during full glacial conditions, and subsequently use the East flowline as our template when considering the sensitivity of the system to different forcing parameters.

During this control experiment, ice thickening at locations adjacent to the Pensacola Mountains ranges from 323 m near Schmidt Hills to 462 m near Thomas Hills (Table S2). The ongoing thickening at the end of the model run (Figure 4, dashed lines) suggests that this experiment does not reach equilibrium.

4.2.2. East Flowline Control Experiment (Experiment A2)

Figure 3b (and Movie S2) depicts the evolution of the FIS after the hypothesized flow-switching has taken place. The grounding line takes ~4500 years from the onset of glacial conditions to advance to a position level with the northern margin of Berkner Island. During the model run, ice thickening at locations adjacent to the Pensacola Mountains ranges from 156 m near Schmidt Hills to 299 m near Thomas Hills, while ice surface elevation increase along the portion of the flowline that passes the Shackleton Range is 113 m (Table S2). Ice *thickness* change at this latter location is much greater than 113 m, because floating ice becomes grounded during the experiment, but it is the change in surface elevation that we are

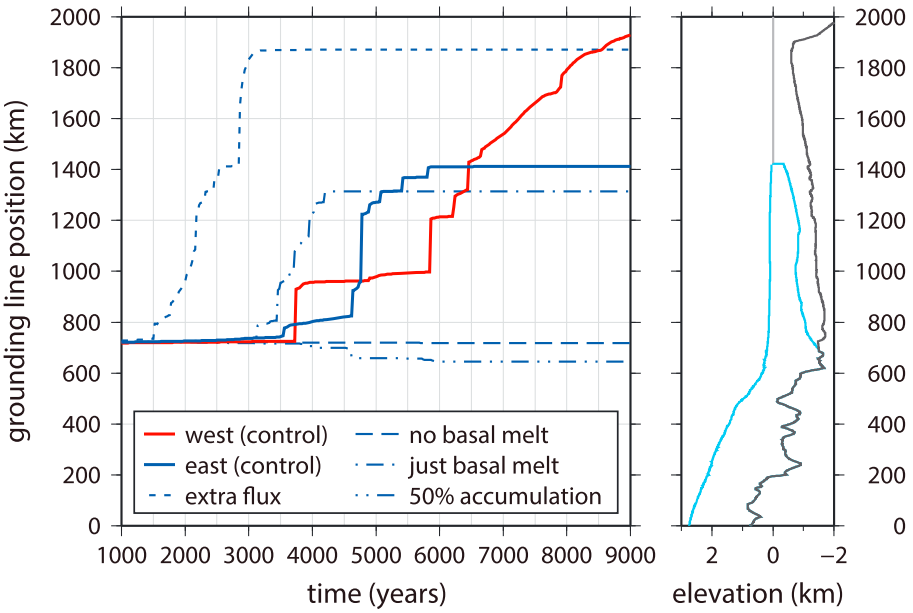

Figure 5. (left) Modeled temporal evolution of grounding line migration in response to the onset of glacial conditions. Initial grounding line location is the observed present-day grounding line location. Apart from the west (control) experiment (A1, Table 3) all experiments refer to the East flowline. In the "no basal melt" experiment (A7, Table 3) all forcing parameters are adjusted to their glacial values except the basal melt parameter. In the "just basal melt" experiment (A4, Table 3) only the basal melt parameter is adjusted to its glacial value. In the "50% accumulation" experiment (A6, Table 3) only the accumulation parameter is adjusted to its glacial value. In the "extra flux" experiment (A9, Table 3) all forcing parameters are adjusted to their glacial values and ice flux from the Institute and Möller ice streams is also included. (right) Profile of the topography and present-day ice stream configuration along the East flowline; downstream distances are again measured from the ice divide.

interested in comparing with observations from the Shackleton Range. Along the whole flowline, ice thickness and elevation changes are negligible during the last ~2000 years of the experiment (Figure 4, solid lines).

4.2.3. Sensitivity Experiments Relating to Grounding Line Advance (Experiments A3–A9)

In addition to simulating full glacial conditions we explore the controls on grounding line advance along the East flowline by altering each of the model parameters individually (Table 3; experiments A3–A6). Our key finding is that basal melt rates play a crucial role in determining whether the grounding line advances along this flowline (Figure 5). The model results suggest that grounding line advance will always take place if the basal melt rates are reduced sufficiently, and it will never take place if they are not. Further investigation (Table 3)—changing all parameters apart from basal melt (experiment A7) or increasing basal melt (experiment A8)—suggests that the maximum basal melt rate must be less than 0.75 m/yr to trigger grounding line advance. Altering each of the other model parameters individually does not result in grounding line advance; indeed, for the case where accumulation rates are decreased the model predicts ~50 km grounding line retreat (Figure 5).

Only one of our experiments produces grounding line advance beyond Berkner Island (experiment A9, Table 3, Figure 3c, and Movie S3); in this case ice flux from the Institute and Möller ice streams is included in the mass balance of the FIS. The early evolution of the experiment is similar to previous experiments in which the grounding line advances to a stable position at the northern margin of Berkner Island. However, around 300 years after the grounding line reaches this point, the ice shelf thickens sufficiently for further grounding to occur in the shallow region just upstream of the continental shelf break. The resulting change in the basal stress profile triggers rapid grounding line advance to the continental shelf break in ~250 years. Predictions for the total amount of ice thickening during this experiment are greater than for experiments where the grounding line does not advance beyond Berkner Island (Figure 6). Ice thickening adjacent to the Pensacola Mountains ranges from 337 m to 494 m (Figure 4, dash-dotted lines), while the ice surface elevation increase downstream from the Shackleton Range is 285 m (Table S2).

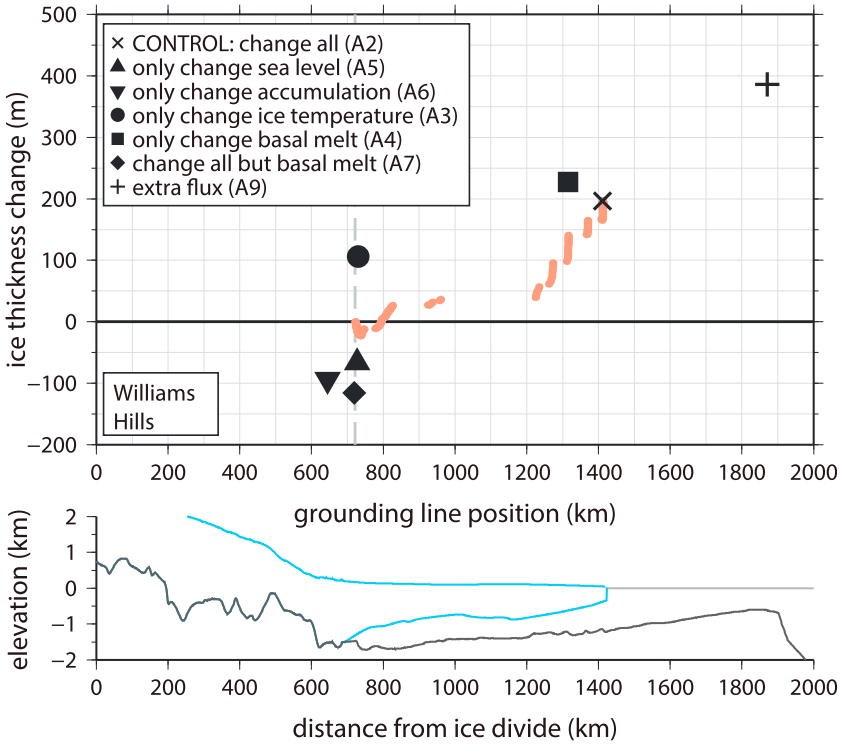

Figure 6. (top) Modeled change in ice thickness adjacent to the Williams Hills for a range of experiments. Net thickness change between the end of spin-up (1000 years) and the end of the experiment (9000 years) is plotted against the final grounding line position in each case. In addition, brown dots show the evolution of thickness change in relation to grounding line migration during the control experiment (A2, Table 3); circles are plotted every 20 years of model time. The vertical grey dashed line represents the present-day/initial grounding line position. All experiments are for the East flowline; experiment numbers (as listed in Table 3) are given in the key. (lower) Topography and ice stream geometry along the East flowline.

In general, we find that the magnitude of the predicted ice thickness increase in the region of the Pensacola Mountains is approximately linearly related to the change in grounding line position (Figure 6). We do not find that the ice thickness continues to increase with time after the grounding line has reached a stable position.

4.3. Response to the Onset of Interglacial Conditions

Output from the final time step of the control experiments described in section 4.2 is used to initiate experiments that explore the response of the FIS to the onset of interglacial conditions. For the East flowline, two initial (glacial) states are used: one in which the grounding line is located adjacent to the northern margin of Berkner Island (final output from experiment A2), and one in which the grounding line is located at the continental shelf break (final output from experiment A9). In addition to varying model parameters from their "glacial" values to their "interglacial" values over 2000 years (Table 2), the magnitude of ice shelf buttressing may also be reduced for a portion of the experiment (see section 3.2).

4.3.1. West Flowline (Experiments R1–R2)

The model is unable to reproduce grounding line retreat along this flowline in response to the onset of interglacial conditions, even if an ~80% reduction in lateral drag is invoked. We hypothesize that the shallow region crossed by this flowline contained stagnant ice during the LGM due to the diversion of streaming ice to the east of Berkner Island, as indicated by the geophysical data. A flowline model based on the shallow shelf approximation is therefore not the appropriate tool for exploring the style of deglaciation in the region west of Berkner Island.

4.3.2. East Flowline (Experiments R3–R6)

The response of the East flowline to the onset of interglacial conditions, for two different initial configurations, is shown in Figure 7. In the case where the initial grounding line is located adjacent to the northern

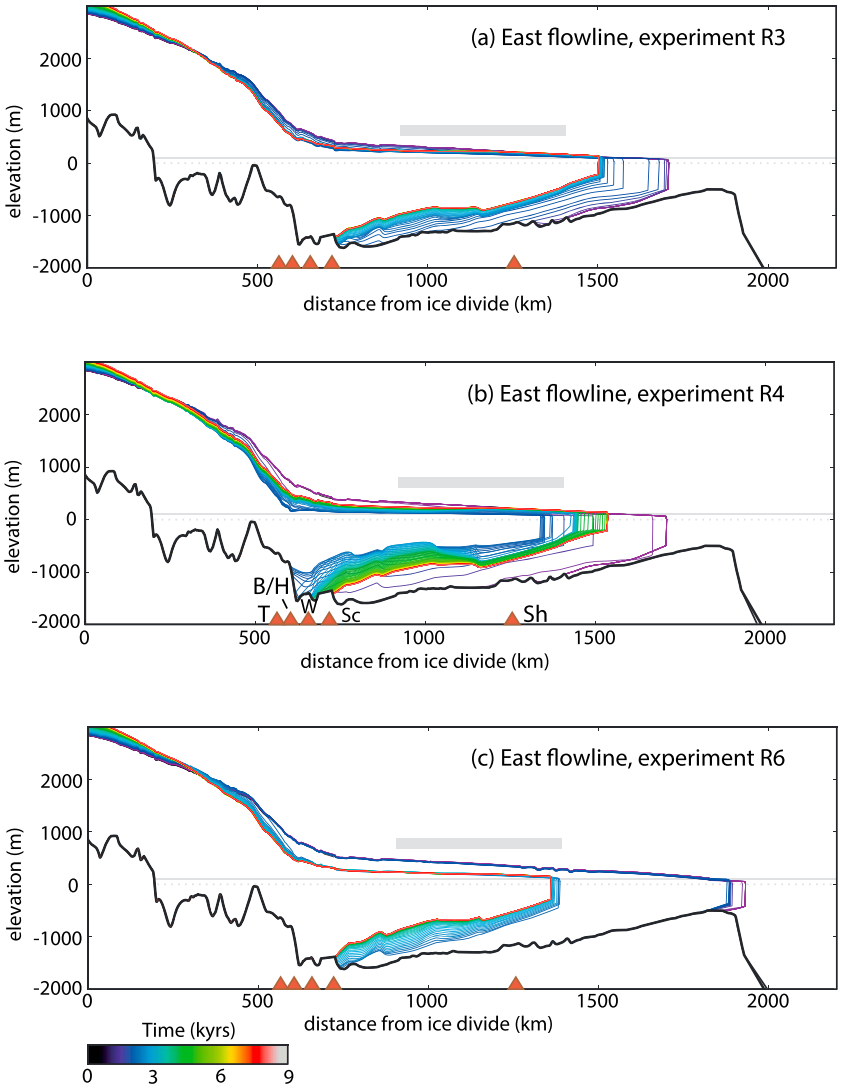

Figure 7. (a) Modeled evolution of ice thickness along the East flowline in response to the onset of interglacial conditions accompanied by an ~50% reduction in ice shelf lateral drag for 1000 years at the start of deglaciation (experiment R3, Table 3). At the start of the model run the grounding line is adjacent to the northern margin of Berkner Island. Model output is shown every 100 years according to the color scale. The horizontal dotted and solid grey lines are the initial and final sea level, respectively, and the approximate extent of Berkner Island is indicated by the horizontal grey bar. Field site locations are indicated on the *x* axis by brown triangles; site names are given in Figure 7b as for Figure 2. (b) As for Figure 7a but for the case of an ~80% reduction in ice shelf lateral drag at the start of deglaciation (experiment R4, Table 3). (c) As for Figure 7b but for the case where the grounding line is located at the continental shelf break at the start of the model run (experiment R6, Table 3).

margin of Berkner Island, a moderate (~50%) reduction in ice shelf buttressing and the onset of interglacial conditions causes the grounding line to retreat to a position ~40 km in front of the present-day grounding line in ~1000 years (Movie S4). The grounding line then stabilizes at this location (Figure 7a; experiment R3). For the case where a significant (~80%) reduction in ice shelf buttressing is invoked (Figure 7b; experiment R4), the grounding line retreats past the present-day grounding line position after ~200 years of reduced buttressing and only stabilizes when it reaches a position ~70 km behind this (Movie S5). After full ice shelf buttressing is reinstated (model time = 2000 years), the grounding line re-advances to stabilize once again just in front of the present-day grounding line position.

For the case where the initial grounding line is located at the continental shelf break, negligible grounding line retreat occurs if there is only a moderate (~50%) reduction in ice shelf buttressing (experiment R5),

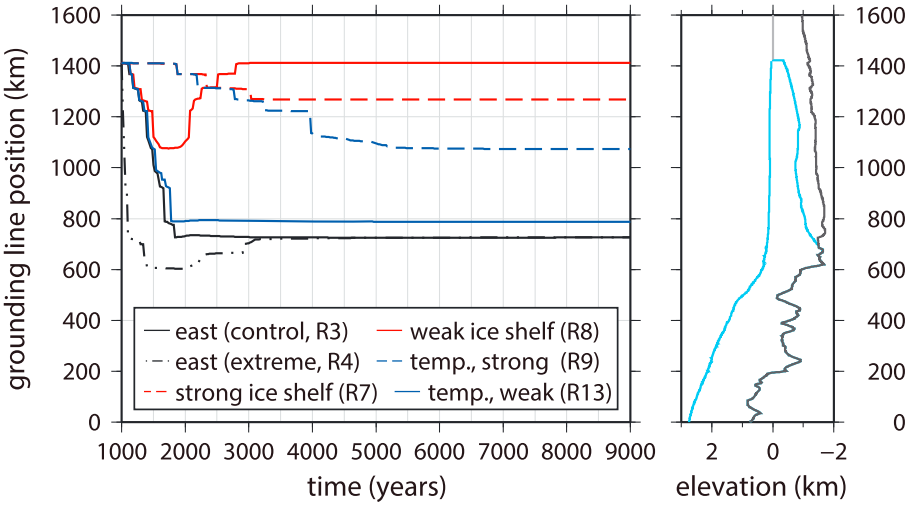

Figure 8. (left) Modeled temporal evolution of grounding line migration in response to the onset of interglacial conditions. All experiments are for the East flowline and at the start of the model run the grounding line lies adjacent to the northern margin of Berkner Island (~1400 km from the ice divide). Model parameters transition from glacial to interglacial values between 1000 and 3000 years (model time). Where relevant, ice shelf lateral drag is only reduced between 1000 and 2000 years. Lateral drag is reduced by ~80% in the "extreme" experiment (R4, Table 3) and ~50% in the "control" experiment (R3, Table 3). In the "strong ice shelf" experiment there is no reduction in lateral drag but all other parameters are varied (R7, Table 3), while in the "weak ice shelf" experiment only a reduction in lateral drag is applied (R8, Table 3). The blue lines show the evolution of the grounding line position when just ice temperature is altered, either with ("weak"; R13, Table 3) or without ("strong"; R9, Table 3) a reduction in ice shelf lateral drag. (right) Profile of the topography and present-day ice stream configuration along the East flowline; distances are measured from the ice divide.

but the grounding line does retreat back to the present-day grounding line position if a significant (~80%) reduction in ice shelf buttressing is invoked (Figure 7c; experiment R6, see also Movie S6). In the latter case, grounding line retreat occurs in two stages, separated by a period of stability. First, as the ice shelf buttressing is reduced, the grounding line retreats ~40 km in 150 years to a position just upstream of the bathymetric high that marks the edge of the continental shelf. The grounding line then stabilizes here for 750 years before rapidly retreating ~1100 km in only 100 years. As in the previous experiments, the grounding line stabilizes ~40 km in front of the present-day grounding line position by the end of the run.

For cases where the grounding line retreats from the northern margin of Berkner Island, net ice thinning in the region of the Pensacola Mountains ranges from 117 m near Schmidt Hills to 225 m near Thomas Hills. If the grounding line was initially located at the continental shelf break then thinning is $>$100 m greater, ranging from 269 m near Schmidt Hills to 384 m near Thomas Hills. Similarly, ice surface elevation decrease downstream of the Shackleton Range is greater for the case where the grounding line is initially located at the continental shelf break: 277 m versus 106 m for the case where the grounding line retreats from the northern margin of Berkner Island (Table S3).

4.3.3. Sensitivity Experiments Relating to Grounding Line Retreat (Experiments R7–R16)

In addition to simulating full interglacial conditions, we explore the controls on grounding line retreat along the East flowline by altering each of the model parameters individually, both with and without a reduction in ice shelf buttressing (Table 3; experiments R9–R16). In these experiments we consider the case where the grounding line is initially located adjacent to the northern margin of Berkner Island. The only single parameter that induces grounding line retreat is an increase in ice temperature, which results in ~300 km of retreat if there is no reduction in ice shelf buttressing, and ~625 km of retreat—almost back to the present-day grounding line position—if there is (Figure 8, blue lines; experiments R9 and R13, respectively). Just changing the maximum basal melt rate or increasing sea level has a negligible cumulative effect on the grounding line position (experiments R10 and R11, respectively): when these parameters are combined with a moderate reduction in ice shelf buttressing this does trigger 300–400 km of grounding line retreat, but re-advance occurs after full ice shelf buttressing is reinstated (experiments R14 and R15). Just increasing accumulation rates back to present-day values results in grounding line advance to the continental shelf break (experiments R12 and R16).

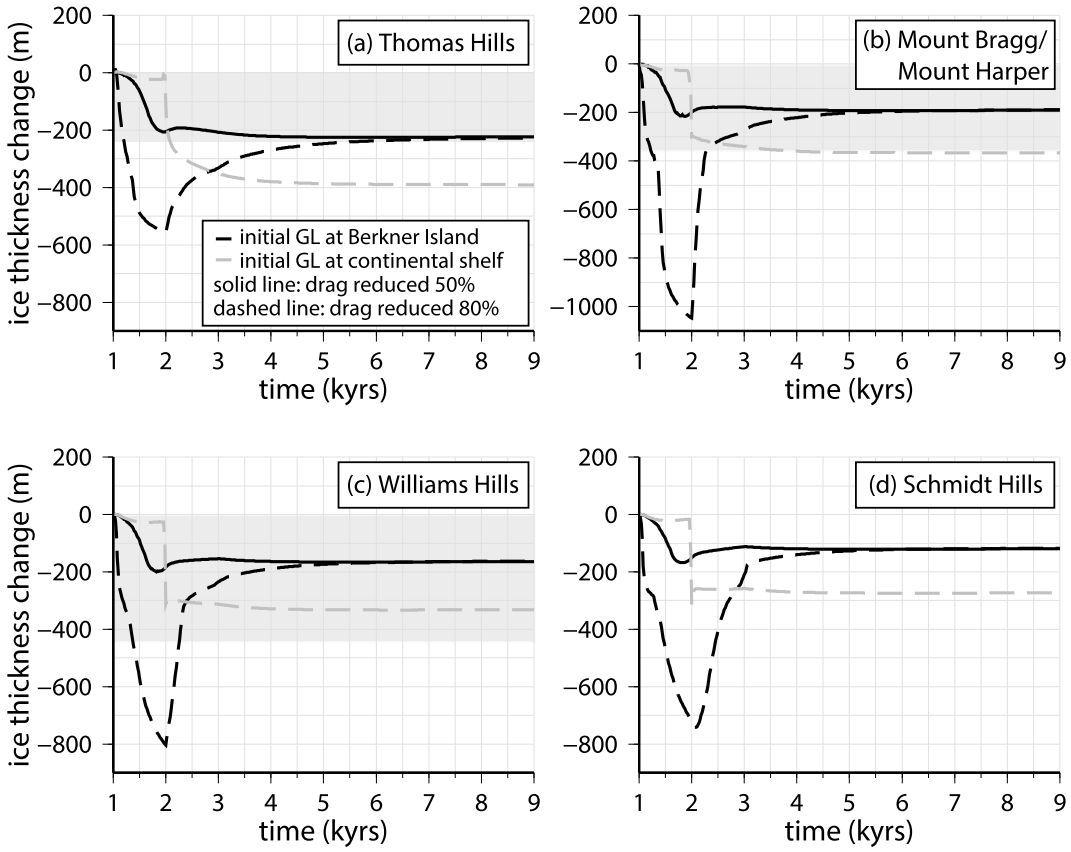

Figure 9. Modeled ice thickness change in response to the onset of interglacial conditions for (a) Thomas Hills, (b) Mount Bragg/Mount Harper, (c) Williams Hills, and (d) Schmidt Hills. The results for three East flowline experiments are shown: the solid black line indicates experiment R3; the dashed black line indicates experiment R4; and the dashed grey line indicates experiment R6. The grey shaded regions indicate the minimum magnitude of ice thinning inferred from the analysis of field data.

In order to investigate the importance of ice shelf buttressing we investigate two further cases: in the case where all of the forcing parameters are varied to simulate a transition to interglacial conditions, but there is no reduction in ice shelf buttressing, the model predicts only slight (~140 km) grounding line retreat (Figure 8, red dashed line; experiment R7). Alternatively, if a reduction in ice shelf buttressing is the only forcing parameter applied (experiment R8), ~330 km of grounding line retreat occurs while ice shelf lateral drag is reduced. However, this is followed by re-advance back to the initial grounding line position after full ice shelf buttressing is reinstated (Figure 8, red solid line). Full grounding line retreat only occurs when we invoke both a reduction in ice shelf buttressing and the onset of interglacial conditions.

Further sensitivity experiments (not shown) suggest that the maximum basal melt rate must be >1 m/yr for the grounding line to retreat back to near the present-day grounding line position. However, although the vertical distribution of basal melt rates affects the shape of the ice shelf, bed topography seems to exert a stronger control on the actual grounding line position. In fact, in all cases where full grounding line retreat occurs, the final grounding line positions all lie within 5 km of each other. This final "grounding zone" lies ~30 km downstream of the stable grounding line position identified in the present-day experiment (section 4.1).

4.3.4. Comparison of Model Predictions With Field Data

Observed and modeled ice thickness changes at four locations in the Pensacola Mountains are shown in Figure 9. All model results relate to the East flowline deglacial experiments described in sections 4.3.2 and 4.3.3. We do not carry out any detailed comparison between the field data and the West flowline experiments apart from noting that modeled advance along this flowline did not reach a state of equilibrium (experiment A1, Figure 5), suggesting that total thickening associated with streaming flow along this flowline would have been greater than the changes predicted by the East flowline experiments.

Our East flowline experiments suggest that if the grounding line retreats behind its present-day position (Figure 9, black dashed lines) >500 m of ice thinning could take place adjacent to the Pensacola Mountains due to the transition from grounded to floating ice. However, in our experiments such a configuration only persists while ice shelf buttressing is reduced by ~80%; soon after full lateral drag is reinstated (after 2000 years of model time) ice thicknesses increase and the grounding line re-advances toward a stable position (Figures 7 and 8). Interestingly, net ice thickness change at each site is the same whether the grounding line retreats behind its eventual final position and then re-advances, or whether it just retreats monotonically to its final position (Figure 9, dashed and solid black lines). At all four sites, the net amount of thinning is 150–175 m greater if the experiment starts from a maximum LGM configuration (grounding line at the continental shelf break) compared with a more restricted LGM configuration (grounding line adjacent to the northern margin of Berkner Island). Differences between these two scenarios are very similar throughout the Pensacola Mountains (Figure 9, black versus grey lines).

The field data at Mount Bragg/Mount Harper, where at least 250 m of thinning is inferred to have taken place in a few thousand years during the late Holocene and 380 m overall since the LLGM [*Bentley et al*., 2016], are best explained by the scenario in which the grounding line was located at the continental shelf break during the LGM (Figure 9b, grey lines). Mount Bragg and Mount Harper do not lie directly adjacent to the FIS (Figure 1b), and so this preference for an advanced grounding line during the LGM relies on the assumption that thinning along the tributary Academy Glacier would have been of a similar magnitude to thinning along the FIS; this point is discussed further in section 5.

Conversely, the field data from Thomas Hills, which suggest >250 m thinning since the LGM (Table 1), are best fit by the scenario in which the LGM grounding line was located at the northern margin of Berkner Island (Figure 9a, black lines). However, since the Thomas Hills data only provide a minimum constraint on post-LGM thinning, they do not rule out the scenario in which the LGM grounding line was located at the continental shelf break. The timing of thinning, as recorded by the field data, is similar at both sites (Table 1). This is consistent with our model results, which predict that thinning in the Pensacola Mountains was essentially synchronous for any given model scenario. The field data at Thomas Hills and Mount Bragg/Mount Harper are not incompatible with a scenario in which the grounding line retreats behind its present-day position during the initial stages of deglaciation, and then re-advances to a stable position.

The simple flowline model underpredicts the magnitude of ice thinning recorded at Williams Hills (>450 m total, and 300 m in the last 7 ka B.P.), even for the scenario in which the LGM grounding line was located at the continental shelf break. In contrast, field data from the Schmidt Hills do not record any post-100 ka B.P. ice thinning [*Balco et al*., 2016]. This is in stark disagreement with the model predictions and may reflect local conditions. Notwithstanding the anomalous evidence from the Schmidt Hills, the fact that the field data from Williams Hills, Thomas Hills, and Mount Bragg/Mount Harper can only constrain the minimal amount of ice thickness change at these sites during the last glacial cycle means that additional evidence is needed to differentiate between scenarios in the which the LGM grounding line reached the northern margin of Berkner Island versus the edge of the continental shelf.

Six hundred kilometers downstream from the Pensacola Mountains, modeled changes in ice surface elevation can be compared with field evidence from the Shackleton Range. This mountain range lies ~200 km from the central flowline being modeled, and it is drained by the Slessor and Recovery Glaciers (Figure 1). The difference in surface elevation along these glaciers, between the Shackleton Range and the Filchner Ice Shelf, is currently ~140 m. *Hein et al*. [2011] found no evidence of ice thickness change along the Shackleton Range portion of the Slessor and Recovery Glaciers since the LGM, and hence, the increase in ice surface elevation along the Filchner Trough during the LGM is inferred to have been ≤140 m, based on current elevation differences. If thickening along the main trough had been any greater then this would have caused the Slessor and Recovery Glaciers to thicken dynamically. Considering the results of our experiments, the field evidence from the Shackleton Range seems to rule out the possibility that the grounding line of the FIS advanced to a stable position at the continental shelf break during the last glacial cycle. However, in contrast to the hypothesis proposed by *Hein et al*. [2011] that ice did not ground beyond the outlet of the Slessor and Recovery Glaciers, we find that ice may have grounded to the northern margin of Berkner Island without contravening the field evidence from the Shackleton Range (Figure 3).

5. Discussion

5.1. Controls on Ice Stream Advance and Retreat

We have used an adapted flowline model to mimic the advance and retreat of the FIS along the Filchner Trough using realistic forcing for the onset of glacial and interglacial conditions, respectively. We find that ice shelf basal melt rates play an important role in controlling grounding line advance and that a reduction in ice shelf buttressing is necessary for grounding line retreat. More generally, the extent, thickness, and coherence of the buttressing ice shelf exert a strong control on FIS dynamics.

FIS sensitivity to realistic changes in ice temperature, sea level, and accumulation is minor, with ice temperature having the greatest relative impact via its influence on the rheology of ice (Figure 8). Changes in sea level alone do not seem to trigger grounding line advance or retreat, although improved knowledge of the bathymetry along the ice stream, particularly in the region of the current grounding line, is required for this result to be considered robust. Feedbacks between ice dynamics and GIA can have a stabilizing effect on grounding line motion, and this should be accounted for in future work, although care must be taken when assigning the response time of the solid Earth as this determines the strength of the coupling [*Gomez et al*., 2015; *Konrad et al*., 2015]. Accumulation changes affect the flux of ice along the ice stream at any time, and while reduced/increased rates of mass input during glacial/interglacial periods would seem to inhibit grounding line advance/retreat, modeling suggests that the other factors discussed above are able to override this. One issue that we cannot satisfactorily explore using the flowline model is whether the total catchment area for the Filchner Trough changes as the whole ice sheet expands or contracts. Several modeling studies suggest that ice from the Institute and Möller ice streams was discharged along the Filchner Trough during the LGM [e.g., *Golledge et al*., 2012; *Whitehouse et al*., 2012a]. We investigate this in one experiment and find that the additional mass flux resulted in the most rapid and extensive grounding line advance of all the experiments (see Figure 6).

One of the most important findings of our study relates to the role of the floating ice shelf in determining when, or even whether, the grounding line of the FIS advances and retreats along the Filchner Trough. In many of the experiments, the principal mechanism of advance or retreat involves the "touchdown" or "lift-off" of the ice shelf on/from a remote bedrock high; in other words, there is a jump in the position of the most offshore location of grounded ice rather than gradual grounding line advance or retreat. Indeed, analysis of the discrepancy between the balance flux and the hypothesized grounding line flux along the East flowline (see section 5.2) indicates that the grounding line is currently in a stable position, and that advance, even under glacial conditions, is unfeasible in the absence of ice shelf buttressing or touchdown. Factors that can lead to ice shelf re-grounding or un-grounding include a change in ice flux, a change in basal melt rate, and a change in the elevation of the bed due to isostatic adjustment. If a floating ice shelf comes into contact with the bed, increased drag at the base of the ice results in the formation of an ice rise or ice rumple. Such features may play an important role in promoting the longevity of existing ice shelves and hence stabilizing the present-day ice sheet [*Matsuoka et al*., 2015]. We find that such features probably also played an important role in determining the rate of grounding line advance and retreat along the Filchner Trough during the last glacial cycle.

5.2. Glacial Expansion and LGM Ice Extent

Most of our experiments explore the behavior of the FIS as it flows along the Filchner Trough, east of Berkner Island. However, ice from the FIS currently flows west of Berkner Island. Our experiments suggest that if this was the main route of ice flux during the LGM, then ice thickening in the Pensacola Mountains would have exceeded the changes determined from cosmogenic nuclide exposure dating (Figure 4, dashed lines). We therefore hypothesize that following grounding on the shallow continental shelf west of Berkner Island, ice preferentially flowed along the deeper Filchner Trough for the majority of the last glacial period. Submarine evidence provides confirmation of past grounded ice flow along the Filchner Trough [*Hillenbrand et al*., 2012; *Larter et al*., 2012], but we currently lack observations from the continental shelf west of Berkner Island. We rule out the scenario in which Berkner Island was completely overridden by ice during the last glacial period because the current elevation difference between Berkner Island and the adjacent ice shelves is ~800 m, while the maximum modeled increase in ice elevation along the adjacent flowlines is only ~280 m and ~320 m, for the East and West flowlines, respectively. This is consistent with independent isotopic evidence from an ice core drilled on Berkner Island [*Mulvaney et al*., 2007].

Our modeling suggests that there are two stable configurations for the FIS in the Filchner Trough under glacial conditions: one in which the grounding line advances to the northern margin of Berkner Island, and one in which the grounding line advances all the way to the continental shelf break. These configurations agree with theoretical steady state configurations for the East flowline, i.e., configurations where the balance flux matches the theoretical steady state flux across the grounding line [*Schoof*, 2007]. Further analysis of the theoretical grounding line flux along the East flowline suggests that there are no stable grounding line positions between the northern margin of Berkner Island and the continental shelf break and that the steady state grounding line position adjacent to the northern margin of Berkner Island owes its existence to small undulations in the bed in this region. In fact, consideration of the forces acting on a grounding line in this position suggests that this is only a steady state configuration in the case where additional buttressing is provided [*Schoof*, 2007, equation (29)], for example, by a laterally confined ice shelf or one that is buttressed by an ice rise. This agrees with our flowline model results, which demonstrate that a loss of ice shelf buttressing can initiate grounding line retreat from this location (experiments R3 and R4). Finally, consideration of the forces acting at the present-day grounding line suggests that the stability of this grounding line also relies on the presence of a buttressing ice shelf; this reflects the behavior seen in experiment R4, in which the grounding line retreated behind the present-day position while ice shelf lateral drag was reduced, before advancing again once full lateral drag was reinstated.

In the case where the grounding line reaches a stable position at the continental shelf break rather than the northern margin of Berkner Island (experiment A9), greater thickening occurs at all points upstream of the grounding line. Comparison with field data suggests that this more extensive scenario is inconsistent with the magnitude of thickening and thinning recorded at some sites in the Pensacola Mountains (Figure 9) and with evidence from the Shackleton Range during the last glacial cycle. This conclusion is reached by comparing the field evidence with the total amount of predicted thickening in the case where the ice stream reaches equilibrium during the LGM. However, analysis of Figures 4 and 5 indicates that the majority of thickening in experiment A9 occurs after the grounding line reaches the continental shelf break. This is in contrast to experiment A2, in which thickening keeps pace with grounding line advance. It is not possible to test whether the rate of grounding line advance in experiment A9 is realistic—some caveats are discussed below—but it is clear that if the LGM grounding line only transiently reached the continental shelf break, or if the ice was so lightly grounded that the increase in basal traction was insufficient to cause upstream thickening [e.g., *Le Brocq et al*., 2011], then such a configuration may be compatible with both the upstream field evidence [*Balco et al*., 2016; *Bentley et al*., 2016] and geophysical evidence from the Filchner Trough [*Larter et al*., 2012].

In the case where the grounding line only reaches the northern margin of Berkner Island, the global mean sea-level contribution due to post-LGM grounding line retreat, only accounting for the changes in the thickness of ice above flotation, would be ~50 mm. Alternatively, if the ice stream reached a stable configuration at the edge of the continental shelf, our modeling suggests that the sea-level contribution would be ~130 mm. Notwithstanding, our inability to predict with confidence the timing of grounding line retreat during the last deglaciation, it is clear that these estimates are insufficient to explain any significant proportion of the sea-level rise observed during MWP-1A.

There are two important caveats to these results, both of which might suggest that a more restricted grounding line position is more likely. First, our modeling does not account for any change in the pattern of accumulation over time. The expansion of the ice sheet during the LGM will have meant that some regions, such as the central Weddell Sea embayment, will have become more distant from the open ocean. This increase in continentality likely led to a greater reduction in accumulation rates in the central Weddell Sea embayment than in other areas of the continent, and consequently, we may have overestimated the flux from the Institute, Möller and Foundation Ice Streams during the LGM. Second, we assume that ice shelf basal melt rates were lower during glacial periods. While this seems to be a necessary condition for grounding line advance, recent modeling suggests that basal melting during full LGM conditions may well have been greater than present, due to the proximity of the extended ice shelves to the continental shelf break, where there is the potential for warm Circumpolar Deep Water to be transported into ice shelf cavities [*Kusahara et al*., 2015]. Such conditions would potentially limit the ability of the grounding line to stabilize at the continental shelf break, adding further weight to the hypothesis that any advance to this position would have been transient.

To summarize, field evidence from the Pensacola Mountains suggests that it is likely that the grounding line of the FIS advanced to at least the northern margin of Berkner Island during the LGM, and this same evidence does not rule out an advance to the shelf edge. However, including evidence from the Shackleton Range, it is unlikely that the grounding line was located at the continental shelf break for an extended period of time. While we can rule out a scenario in which grounded ice extended to the continental shelf break for a prolonged period, it is not possible to determine the duration that the grounding line may have been located adjacent to Berkner Island for two reasons. (i) Our model suggests that it is possible for ice thickening in the Pensacola Mountains to keep pace with grounding line advance, and therefore, it is not necessary for the grounding line to stabilize for a given period of time before maximum thicknesses are transiently reached. (ii) Similarly, ice thicknesses do not further increase once the grounding line stabilizes, and therefore, we cannot determine a maximum duration for this ice stream configuration.

5.3. Ice Retreat and Ice Stream Reorganization

The model fails to reproduce grounding line retreat from the continental shelf break for the West flowline, even under conditions of significantly reduced ice shelf buttressing (experiments R1 and R2). This is not surprising because the length of the ice shelf in this maximum configuration is short relative to the total length of the flowline, and therefore, reducing lateral drag only along the ice shelf is insufficient to trigger grounding line retreat across the broad, shallow continental shelf north of Berkner Island.

In contrast, the model is able to reproduce grounding line retreat for the East flowline scenario, both from the northern margin of Berkner Island (experiments R3 and R4) and from the continental shelf break (experiment R6). For this latter scenario, an ~80% reduction in ice shelf buttressing is necessary to trigger grounding line retreat. Initially, the grounding line only retreats to the southern margin of the topographic high which forms the continental shelf break (Figure 7c). However, the bed deepens inland of this point so this is an unstable grounding line position for the case where ice shelf buttressing is negligible [*Weertman*, 1974]. As sea level continues to rise, ice temperatures increase (causing ice to flow faster), and basal melt increases (reducing buttressing), the East flowline system is eventually destabilized, resulting in rapid grounding line retreat back to the present-day position in only 100 years. Based on an analysis of geomorphological features near the edge of the continental shelf, *Larter et al*. [2012] also propose that the main deglacial retreat from the continental shelf break was preceded by an initial retreat of $<$100 km, in agreement with our modeling. Furthermore, the location at which our modeled grounding line pauses for ~750 years just upstream of the continental shelf break agrees closely with the location of the grounding zone wedge identified by *Larter et al*. [2012].

Our treatment of ice shelf debuttressing is parameterized within the model rather than being dynamically determined and may overestimate the magnitude and rate at which debuttressing of a whole ice shelf could occur, but our results raise important questions regarding ice shelf dynamics during deglaciation. For example, how extensively and how quickly could a large floating ice shelf become weakened to the degree that it provides negligible buttressing to ice behind the grounding line? How quickly could an ice shelf re-form? Iceberg furrows provide some evidence for past ice shelf disintegration within the Filchner Trough [*Larter et al*., 2012], but the dating of such an event is problematic, and additional age constraints should be sought, for example, by seeking to attribute ice-rafted debris recovered from marine sediment cores to this outlet of the Antarctic Ice Sheet. If the source of ice-rafted debris [e.g., *Weber et al*., 2014] can be determined this will allow better constraints to be placed on the timing of large iceberg discharge events from specific regions of the ice sheet. Although this does not provide a constraint on the change in grounded ice volume, it could provide important information on the dynamics of specific ice streams feeding the ice shelves during the past.

Following grounding line retreat behind present, our model predicts re-advance to its present position once full ice shelf buttressing is re-established. This preference for the grounding line to be located close to its current position is in line with the findings of *Wright et al*. [2014], who concluded that realistic increases in basal melt are unable to trigger retreat from the present grounding line position, suggesting that the grounding line is currently in a stable position. Our modeling also suggests that net post-LGM ice thickness change in the region of the Pensacola Mountains would be the same whether or not the grounding line retreated behind present during the Holocene (Figure 9). Due to the similarity of the final ice stream profile in experiments R3 and R4 we are therefore unable to determine which scenario is more likely, based on

current field constraints. Exposure dating of material beneath the current ice sheet would provide crucial evidence relating to past ice sheet configuration, and in this context would also provide constraints on past ice shelf conditions along the Filchner Trough.

One issue that we are unable to explore using a flowline model is the time at which ice switched from flowing east of Berkner Island during the LGM to flowing west of Berkner Island at the present. *Siegert et al*. [2013] presented independent evidence for flow re-organization in the south-east Weddell Sea within the last ~4000 years, and this is consistent with evidence from the southern Ellsworth Mountains where *Hein et al*. [2016] argued for a reorganization of ice flow between 6.5 and 3.5 ka B.P.. The timing and details of such a reconfiguration should be explored by using a 3-D model.

5.4. Past Ice Dynamics in the Pensacola Mountains

There are several aspects to the field data from the Pensacola Mountains that cannot be explained by our modeling. First, cosmogenic nuclide exposure dating in the Schmidt Hills provides no evidence for ice cover in the last 100 ka B.P., while our modeling suggests that the FIS in this region was at least 100 m thicker during the LGM (Figure 9). One explanation for this may be that this range has experienced a complex exposure history and was only briefly covered by cold-based, debris-poor ice during the last glacial cycle. For example, if the Childs Glacier expanded during the last glacial cycle then this could have led to a debris-poor, locally derived flowline passing across the Schmidt Hills rather than ice from the FIS itself [*Bentley et al*., 2016]. Alternatively, we note that the lowest exposed slopes of the Schmidt Hills currently lie ~100 m above the surface of the main FIS, and hence, up to 100 m thickening could occur along the FIS without this being recorded by the adjacent outcrops. These two factors make it difficult for evidence from this outcrop to be used to constrain past ice stream behavior.

In contrast, Thomas Hills and Mount Bragg/Mount Harper lie at very similar elevations to the main trunk of the FIS and the Academy Glacier, respectively. Comparison of modeled ice thickness change with cosmogenic nuclide exposure data from these ranges therefore provides a more direct constraint on past ice stream dynamics, assuming that thinning along the Academy Glacier was of a similar magnitude to thinning along the FIS. The magnitude of thinning recorded at both Thomas Hills and Mount Bragg/Mount Harper is greater than the scenario in which the grounding line stabilized at the northern margin of Berkner Island during the last glacial cycle (Figure 9; noting that data from Thomas Hills only provide a minimum constraint on the total magnitude of thinning since the LGM). The magnitude of post-LGM thinning recorded in the Williams Hills is greater than the magnitude of thickness change predicted by any of our experiments. We hypothesize that ice from the Academy Glacier (Figure 1) may have been diverted into the embayment containing the Williams Hills during the LGM, leading to localized thickening.

There are no further outcrops upstream of the Pensacola Mountains against which to test our modeling output. However, we note that the main retreat experiments (R3, R4, and R6; Figure 7) predict ice thickening in the upper few hundred kilometers of the flowline during the transition from glacial to interglacial conditions, in contrast to thinning at lower elevations. This is in agreement with evidence from the Vostok and Dome Fuji ice cores in central East Antarctica, which indicate ~150 m ice thickening across the East Antarctic plateau since the LGM [*Parrenin et al*., 2007].

5.5. Limitations of This Study and Implications for Future Work

We are confident that the results presented here provide realistic estimates for the magnitude of ice thickening and thinning along the Filchner Trough during the last glacial cycle. Our use of a flowline model allows us to explore ice stream behavior at high resolution, in response to a large suite of forcing parameters, over multimillennial periods, and hence, our results provide useful information regarding the sensitivity of the FIS to a range of potential controls. However, this study has a number of limitations, including the assumption that the ice stream is isothermal; the neglect of isostasy; the parameterization of basal melting, basal traction, and lateral drag; the lack of consideration of subglacial or surface meltwater; and the fact that the model does not use a physically based calving law to moderate ice shelf length. These last two factors potentially play an important role in controlling the rate of ice sheet retreat [*Pollard et al*., 2015]. The majority of these limitations also apply to 3-D models.

Poor constraints on various boundary conditions also limit our ability to accurately reconstruct past ice stream behavior. In particular, more accurate bathymetry and a better constraints on past accumulation rates

and ocean temperatures would enable us to investigate the timing and rate of past ice sheet change more accurately. The temperature of ocean water that came into contact with the FIS during the last glacial cycle, and hence the distribution of basal melt, depends on the pattern of circulation in the ice shelf cavity. Sub-ice-shelf circulation throughout the Weddell Sea is likely to have been very different during periods when grounding line advance meant that water could not circulate south of Berkner Island.

The original motivation for developing the flowline model used in this study was to accurately track FIS grounding line migration, but our results also highlight the importance of modeling ice shelf dynamics when seeking to understand grounding line behavior. We acknowledge that ice flow in the south-east Weddell Sea is far from simple and that ice stream trajectories were likely different in the past, and therefore suggest that the precise controls on grounding line advance and retreat along the Filchner Trough should be further explored with models that include a more realistic treatment of ice shelf dynamics and can account for the 3-D evolution of ice dynamics.

6. Conclusions

We investigate the controls on advance and retreat of the Foundation Ice Stream (FIS) grounding line along the Filchner Trough, under the onset of glacial and interglacial conditions, using a numerical flowline model. We compare our results with geomorphological observations relating to ice extent and thickness change during the last glacial cycle, and draw the following conclusions:

1. Sensitivity experiments suggest that the present-day grounding line of the FIS is in a stable position, as long as the buttressing Filchner-Ronne Ice Shelf persists.
2. Our modeling suggests that a reduction in ice shelf basal melt plays an important role in triggering grounding line advance along the Filchner Trough and that a reduction in ice shelf buttressing may be a necessary condition for grounding line retreat. In general, ice shelf processes, including the formation of ice rises and ice rumples, exert a strong control on ice dynamics in this region.
3. The flowline modeling indicates two stable LGM grounding line positions: at the northern margin of Berkner Island and at the edge of the continental shelf. This result is supported by a flux analysis of steady state grounding line positions along the Filchner Trough.
4. Our model predicts grounding line advance to the edge of the continental shelf only if we assume that the Institute and Möller Ice Streams were tributaries of the FIS during the LGM.
5. When compared with model predictions of ice thickness change, recent field evidence from the Pensacola Mountains cannot robustly discriminate between the two LGM grounding line scenarios. We also note that the data are not inconsistent with a scenario in which the grounding line retreated behind its present position during the Holocene.
6. Cosmogenic nuclide evidence suggesting negligible ice thickening in the Shackleton Range is incompatible with a scenario in which the grounding line of the FIS reached a long-term, steady state position at the edge of the continental shelf during the LGM. However, a transient advance to this position, accommodated by lightly grounded streaming ice, is compatible with the model results, cosmogenic nuclide data, and submarine field evidence.
7. The global mean sea-level contribution from the FIS since the LGM, only accounting for the change in ice thickness above flotation, was likely ~50 mm if the grounding line reached the northern margin of Berkner Island, and ~130 mm if it reached a stable configuration at the edge of the continental shelf.
8. Sensitivity experiments suggest that the magnitude of buttressing provided by the ice shelf plays a key role in governing the dynamics of the FIS. Constraints on past ocean forcing are therefore needed to better understand the ice shelf processes that were operating in this region during the last glacial cycle.

Acknowledgments
This work was funded by NERC grants NE/F014260/1, NE/F014252/1, and NE/J018333/1. Some data used in this paper were acquired by NASA's Operation IceBridge Project. All of the data supporting our conclusions are contained in tables in the main text and supporting information document. Additional materials are available on request from the corresponding author. The authors are grateful to Richard Hindmarsh for insightful discussions that led to significant improvements being made to an early draft of the manuscript, and we thank two anonymous reviewers and the Editor for their constructive feedback during the review process.

References

Anderson, J. B., S. S. Shipp, A. L. Lowe, J. S. Wellner, and A. B. Mosola (2002), The Antarctic Ice Sheet during the Last Glacial Maximum and its subsequent retreat history: A review, *Quat. Sci. Rev.*, *21*(1-3), 49–70.

Arthern, R. J., D. P. Winebrenner, and D. G. Vaughan (2006), Antarctic snow accumulation mapped using polarization of 4.3-cm wavelength microwave emission, *J. Geophys. Res.*, *111*, D06107, doi:10.1029/2004JD005667.

Balco, G., C. Todd, K. Huybers, S. Campbell, M. Vermuelen, B. M. Goehring, and T. R. Hillebrand (2016), Cosmogenic-nuclide exposure ages from the Pensacola Mountains adjacent to the Foundation Ice Stream, Antarctica, *Am. J. Sci.*, *316*, 542–577, doi:10.2475/06.2016.02.

Bentley, M. J. (1999), Volume of Antarctic Ice at the Last Glacial Maximum, and its impact on global sea level change, *Quat. Sci. Rev.*, *18*(14), 1569–1595.

Bentley, M. J., C. J. Fogwill, A. M. Le Brocq, A. L. Hubbard, D. E. Sugden, T. J. Dunai, and S. P. H. T. Freeman (2010), Deglacial history of the West Antarctic Ice Sheet in the Weddell Sea embayment: Constraints on past ice volume change, *Geology*, *38*(5), 411–414, doi:10.1130/G30754.1.

Bentley, M. J., et al. (2014), A community-based geological reconstruction of Antarctic Ice Sheet deglaciation since the Last Glacial Maximum, *Quat. Sci. Rev.*, *100*, 1–9, doi:10.1016/j.quascirev.2014.06.025.

Bentley, M. J., A. S. Hein, D. E. Sugden, P. L. Whitehouse, R. Shanks, S. Xu, and S. P. H. T. Freeman (2016), Deglacial history of the Pensacola Mountains, Antarctica from glacial geomorphology and cosmogenic nuclide surface exposure dating, *Quat. Sci. Rev.*, doi:10.1016/j.quascirev.2016.09.028.

Bingham, R. G., D. M. Rippin, N. B. Karlsson, H. F. J. Corr, F. Ferraccioli, T. A. Jordan, A. M. Le Brocq, K. C. Rose, N. Ross, and M. J. Siegert (2015), Ice-flow structure and ice dynamic changes in the Weddell Sea sector of West Antarctica from radar-imaged internal layering, *J. Geophys. Res. Earth Surf*, *120*, 655–670, doi:10.1002/2014JF003291.

Bradley, S. L., R. C. A. Hindmarsh, P. L. Whitehouse, M. J. Bentley, and M. A. King (2015), Low post-glacial rebound rates in the Weddell Sea due to Late Holocene ice-sheet readvance, *Earth Planet. Sci. Lett.*, *413*, 79–89, doi:10.1016/j.epsl.2014.12.039.

Briggs, R. D., D. Pollard, and L. Tarasov (2014), A data-constrained large ensemble analysis of Antarctic evolution since the Eemian, *Quat. Sci. Rev.*, *103*, 91–115, doi:10.1016/j.quascirev.2014.09.003.

Clark, P. U., A. S. Dyke, J. D. Shakun, A. E. Carlson, J. Clark, B. Wohlfarth, J. X. Mitrovica, S. W. Hostetler, and A. M. McCabe (2009), The Last Glacial Maximum, *Science*, *325*(5941), 710–714.

Cuffey, K. M., and W. S. B. Paterson (2010), *The Physics of Glaciers*, 4th ed., Butterworth-Heinemann.

Deschamps, P., N. Durand, E. Bard, B. Hamelin, G. Camoin, A. L. Thomas, G. M. Henderson, J. Okuno, and Y. Yokoyama (2012), Ice-sheet collapse and sea-level rise at the Bolling warming 14,600 years ago, *Nature*, *483*(7391), 559–564, doi:10.1038/Nature10902.

Dupont, T. K., and R. B. Alley (2005), Assessment of the importance of ice-shelf buttressing to ice-sheet flow, *Geophys. Res. Lett.*, *32*, L04503, doi:10.1029/2004GL022024.

Farrell, W. E., and J. A. Clark (1976), On postglacial sea level, *Geophys. J. R. Astron. Soc.*, *46*(3), 647–667.

Fretwell, P., et al. (2013), Bedmap2: Improved ice bed, surface and thickness datasets for Antarctica, *Cryosphere*, *7*, 375–393.

Glasser, N. F., S. J. A. Jennings, M. J. Hambrey, and B. Hubbard (2015), Origin and dynamic significance of longitudinal structures ("flow stripes") in the Antarctic Ice Sheet, *Earth Surf. Dyn.*, *3*(2), 239–249, doi:10.5194/esurf-3-239-2015.

Glen, J. W. (1955), The creep of polycrystalline ice, *Proc. R. Soc. London, Ser. A*, *228*(1175), 519–538, doi:10.1098/rspa.1955.0066.

Gogineni, P. (2012), *CReSIS Radar Depth Souder Data*, Digital Media, Lawrence, Kansas. [Available at http://data.cresis.ku.edu/.]

Golledge, N. R., C. J. Fogwill, A. N. Mackintosh, and K. M. Buckley (2012), Dynamics of the Last Glacial Maximum Antarctic ice-sheet and its response to ocean forcing, *Proc. Natl. Acad. Sci. U.S.A.*, doi:10.1073/pnas.1205385109.

Golledge, N. R., et al. (2013), Glaciology and geological signature of the Last Glacial Maximum Antarctic ice sheet, *Quat. Sci. Rev.*, *78*, 225–247, doi:10.1016/j.quascirev.2013.08.011.

Golledge, N. R., L. Menviel, L. Carter, C. J. Fogwill, M. H. England, G. Cortese, and R. H. Levy (2014), Antarctic contribution to meltwater pulse 1A from reduced Southern Ocean overturning, *Nat. Commun.*, *5*, 5107, doi:10.1038/Ncomms6107.

Gomez, N., J. X. Mitrovica, P. Huybers, and P. U. Clark (2010), Sea level as a stabilizing factor for marine-ice-sheet grounding lines, *Nat. Geosci.*, *3*(12), 850–853, doi:10.1038/Ngeo1012.

Gomez, N., D. Pollard, and J. X. Mitrovica (2013), A 3-D coupled ice sheet-sea level model applied to Antarctica through the last 40 ky, *Earth Planet. Sci. Lett.*, *384*, 88–99.

Gomez, N., D. Pollard, and D. Holland (2015), Sea-level feedback lowers projections of future Antarctic Ice-Sheet mass loss, *Nat. Commun.*, *6*, doi:10.1038/ncomms9798.

Greischar, L. L., and C. R. Bentley (1980), Isostatic equilibrium grounding line between the West Antarctic inland ice-sheet and the Ross ice shelf, *Nature*, *283*(5748), 651–654.

Gudmundsson, G. H. (2013), Ice-shelf buttressing and the stability of marine ice sheets, *Cryosphere*, *7*(2), 647–655, doi:10.5194/tc-7-647-2013.

Hall, B. L., G. H. Denton, S. L. Heath, M. S. Jackson, and T. N. B. Koffman (2015), Accumulation and marine forcing of ice dynamics in the western Ross Sea during the last deglaciation, *Nat. Geosci.*, *8*(8), 625–628, doi:10.1038/Ngeo2478.

Hein, A. S., C. J. Fogwill, D. E. Sugden, and S. Xu (2011), Glacial/interglacial ice-stream stability in the Weddell Sea embayment, Antarctica, *Earth Planet. Sci. Lett.*, *307*, 211–221.

Hein, A. S., S. M. Marrero, J. Woodward, S. A. Dunning, K. Winter, M. J. Westoby, S. P. H. T. Freeman, R. P. Shanks, and D. E. Sugden (2016), Mid-Holocene pulse of thinning in the Weddell Sea sector of the West Antarctic ice sheet, *Nat. Commun.*, *7*, 12511, doi:10.1038/ncomms12511.

Hellmer, H. H., F. Kauker, R. Timmermann, J. Determann, and J. Rae (2012), Twenty-first-century warming of a large Antarctic ice-shelf cavity by a redirected coastal current, *Nature*, *485*(7397), 225–228, doi:10.1038/nature11064.

Hillenbrand, C. D., M. Melles, G. Kuhn, and R. D. Larter (2012), Marine geological constraints for the grounding-line position of the Antarctic Ice Sheet on the southern Weddell Sea shelf at the Last Glacial Maximum, *Quat. Sci. Rev.*, *32*, 25–47, doi:10.1016/j.quascirev.2011.11.017.

Hillenbrand, C. D., et al. (2014), Reconstruction of changes in the Weddell Sea sector of the Antarctic Ice Sheet since the Last Glacial Maximum, *Quat. Sci. Rev.*, *100*, 111–136, doi:10.1016/j.quascirev.2013.07.020.

Huybrechts, P., O. Rybak, F. Pattyn, U. Ruth, and D. Steinhage (2007), Ice thinning, upstream advection, and non-climatic biases for the upper 89% of the EDML ice core from a nested model of the Antarctic ice sheet, *Clim. Past*, *3*(4), 577–589.

Jamieson, S. S. R., A. Vieli, S. J. Livingstone, C. O. Cofaigh, C. Stokes, C. D. Hillenbrand, and J. A. Dowdeswell (2012), Ice-stream stability on a reverse bed slope, *Nat. Geosci.*, *5*(11), 799–802, doi:10.1038/Ngeo1600.

Jamieson, S. S. R., A. Vieli, C. O. Cofaigh, C. R. Stokes, S. J. Livingstone, and C. D. Hillenbrand (2014), Understanding controls on rapid ice-stream retreat during the last deglaciation of Marguerite Bay, Antarctica, using a numerical model, *J. Geophys. Res. Earth Surf.*, *119*, 247–263, doi:10.1002/2013JF002934.

Jenkins, A. (1991), A one-dimensional model of ice shelf-ocean interaction, *J. Geophys. Res.*, *96*(C11), 20,671–20,677, doi:10.1029/91JC01842.

Joughin, I., and R. B. Alley (2011), Stability of the West Antarctic ice sheet in a warming world, *Nat. Geosci.*, *4*(8), 506–513, doi:10.1038/Ngeo1194.

Joughin, I., J. L. Bamber, T. Scambos, S. Tulaczyk, M. Fahnestock, and D. R. MacAyeal (2006), Integrating satellite observations with modelling: Basal shear stress of the Filcher-Ronne ice streams, Antarctica, *Proc. R. Soc. London, Ser. A*, *364*(1844), 1795–1814, doi:10.1098/rsta.2006.1799.

Konrad, H., I. Sasgen, D. Pollard, and V. Klemann (2015), Potential of the solid-Earth response for limiting long-term West Antarctic Ice Sheet retreat in a warming climate, *Earth Planet. Sci. Lett.*, *432*, 254–264, doi:10.1016/j.epsl.2015.10.008.

Kusahara, K., T. Sato, A. Oka, T. Obase, R. Greve, A. Abe-Ouchi, and H. Hasumi (2015), Modelling the Antarctic marine cryosphere at the Last Glacial Maximum, *Ann. Glaciol.*, *56*(69), 425–435, doi:10.3189/2015AoG69A792.

Larter, R. D., A. G. C. Graham, C. D. Hillenbrand, J. A. Smith, and J. A. Gales (2012), Late Quaternary grounded ice extent in the Filchner Trough, Weddell Sea, Antarctica: New marine geophysical evidence, *Quat. Sci. Rev.*, *53*, 111–122, doi:10.1016/j.quascirev.2012.08.006.

Le Brocq, A. M., M. J. Bentley, A. Hubbard, C. J. Fogwill, D. E. Sugden, and P. L. Whitehouse (2011), Reconstructing the Last Glacial Maximum ice sheet in the Weddell Sea embayment, Antarctica, using numerical modelling constrained by field evidence, *Quat. Sci. Rev.*, *30*(19-20), 2422–2432, doi:10.1016/j.quascirev.2011.05.009.

Le Brocq, A. M., et al. (2013), Evidence from ice shelves for channelized meltwater flow beneath the Antarctic Ice Sheet, *Nat. Geosci.*, *6*(11), 945–948, doi:10.1038/Ngeo1977.

Makinson, K., P. R. Holland, A. Jenkins, K. W. Nicholls, and D. M. Holland (2011), Influence of tides on melting and freezing beneath Filchner-Ronne Ice Shelf, Antarctica, *Geophys. Res. Lett.*, *38*, L06601, doi:10.1029/2010GL046462.

Maris, M. N. A., B. de Boer, S. R. M. Ligtenberg, M. Crucifix, W. J. van de Berg, and J. Oerlemans (2014), Modelling the evolution of the Antarctic ice sheet since the last interglacial, *Cryosphere*, *8*(4), 1347–1360, doi:10.5194/tc-8-1347-2014.

Matsuoka, K., et al. (2015), Antarctic ice rises and rumples: Their properties and significance for ice-sheet dynamics and evolution, *Earth Sci. Rev.*, *150*, 724–745.

Mengel, M., J. Feldmann, and A. Levermann (2016), Linear sea-level response to abrupt ocean warming of major West Antarctic ice basin, *Nat. Clim. Change*, *6*, 71–74.

Mulvaney, R., C. Arrowsmith, J. Barnola, T. McCormack, L. Loulergue, D. Raynaud, V. Lipenkov, and R. Hindmarsh (2007), A deglaciation climate and ice sheet history of the Weddell Sea region from the Berkner Island ice core, *Quat. Int.*, *167-168*, 294–295.

Nick, F. M., A. Vieli, I. M. Howat, and I. Joughin (2009), Large-scale changes in Greenland outlet glacier dynamics triggered at the terminus, *Nat. Geosci.*, *2*(2), 110–114, doi:10.1038/Ngeo394.

Parrenin, F., et al. (2007), 1-D-ice flow modelling at EPICA Dome C and Dome Fuji, East Antarctica, *Clim. Past*, *3*(2), 243–259.

Pattyn, F., et al. (2012), Results of the Marine Ice Sheet Model Intercomparison Project, MISMIP, *Cryosphere*, *6*(3), 573–588, doi:10.5194/tc-6-573-2012.

Pollard, D., and R. M. DeConto (2012), Description of a hybrid ice sheet-shelf model, and application to Antarctica, *Geosci. Model Dev.*, *5*(5), 1273–1295, doi:10.5194/gmd-5-1273-2012.

Pollard, D., R. M. DeConto, and R. B. Alley (2015), Potential Antarctic Ice Sheet retreat driven by hydrofracturing and ice cliff failure, *Earth Planet. Sci. Lett.*, *412*, 112–121, doi:10.1016/j.epsl.2014.12.035.

Rignot, E., J. L. Bamber, M. R. Van Den Broeke, C. Davis, Y. H. Li, W. J. Van De Berg, and E. Van Meijgaard (2008), Recent Antarctic ice mass loss from radar interferometry and regional climate modelling, *Nat. Geosci.*, *1*(2), 106–110, doi:10.1038/Ngeo102.

Rignot, E., J. Mouginot, and B. Scheuchl (2011), Ice flow of the Antarctic Ice Sheet, *Science*, *333*(6048), 1427–1430, doi:10.1126/science.1208336.

Ross, N., R. G. Bingham, H. F. J. Corr, F. Ferraccioli, T. A. Jordan, A. Le Brocq, D. M. Rippin, D. Young, D. D. Blankenship, and M. J. Siegert (2012), Steep reverse bed slope at the grounding line of the Weddell Sea sector in West Antarctica, *Nat. Geosci.*, *5*(6), 393–396, doi:10.1038/Ngeo1468.

Schoof, C. (2007), Ice sheet grounding line dynamics: Steady states, stability, and hysteresis, *J. Geophys. Res.*, *112*, F03S28, doi:10.1029/2006JF000664.

Siegert, M. J. (2003), Glacial-interglacial variations in central East Antarctic ice accumulation rates, *Quat. Sci. Rev.*, *22*(5-7), 741–750, doi:10.1016/S0277-3791(02)00191-9.

Siegert, M., N. Ross, H. Corr, J. Kingslake, and R. Hindmarsh (2013), Late Holocene ice-flow reconfiguration in the Weddell Sea sector of West Antarctica, *Quat. Sci. Rev.*, *78*, 98–107, doi:10.1016/j.quascirev.2013.08.003.

Smith, B. E., H. A. Fricker, I. R. Joughin, and S. Tulaczyk (2009), An inventory of active subglacial lakes in Antarctica detected by ICESat (2003–2008), *J. Glaciol.*, *55*(192), 573–595.

Stolldorf, T., H. W. Schenke, and J. B. Anderson (2012), LGM ice sheet extent in the Weddell Sea: Evidence for diachronous behavior of Antarctic Ice Sheets, *Quat. Sci. Rev.*, *48*, 20–31, doi:10.1016/j.quascirev.2012.05.017.

Thoma, M., J. Determann, K. Grosfeld, S. Goeller, and H. H. Hellmer (2015), Future sea-level rise due to projected ocean warming beneath the Filchner Ronne Ice Shelf: A coupled model study, *Earth Planet. Sci. Lett.*, *431*, 217–224, doi:10.1016/j.epsl.2015.09.013.

Thomas, R. H., and C. R. Bentley (1978), Model for Holocene retreat of West Antarctic Ice Sheet, *Quat. Res.*, *10*(2), 150–170, doi:10.1016/0033-5894(78)90098-4.

Timmermann, R., et al. (2010), A consistent data set of Antarctic ice sheet topography, cavity geometry, and global bathymetry, *Earth Syst. Sci. Data*, *2*, 261–273, doi:10.5194/essd-2-261-2010.

Van der Veen, C. J., and I. M. Whillans (1996), Model experiments on the evolution and stability of ice streams, *Ann. Glaciol.*, *23*, 129–137.

Vieli, A., and A. J. Payne (2005), Assessing the ability of numerical ice sheet models to simulate grounding line migration, *J. Geophys. Res.*, *110*, F01003, doi:10.1029/2004JF000202.

Weber, M. E., et al. (2014), Millennial-scale variability in Antarctic ice-sheet discharge during the last deglaciation, *Nature*, *510*(7503), 134–138, doi:10.1038/nature13397.

Weertman, J. (1957), On the sliding of glaciers, *J. Glaciol.*, *3*, 33–38.

Weertman, J. (1974), Stability of the junction of an ice sheet and an ice shelf, *J. Glaciol.*, *13*(67), 3–13.

Whitehouse, P. L., M. J. Bentley, and A. M. Le Brocq (2012a), A deglacial model for Antarctica: Geological constraints and glaciological modelling as a basis for a new model of Antarctic glacial isostatic adjustment, *Quat. Sci. Rev.*, *32*, 1–24.

Whitehouse, P. L., M. J. Bentley, G. A. Milne, M. A. King, and I. D. Thomas (2012b), A new glacial isostatic adjustment model for Antarctica: Calibrating the deglacial model using observations of relative sea-level and present-day uplift rates, *Geophys. J. Int.*, *190*, 1464–1482, doi:10.1111/j.1365-246X.2012.05557.x.

Winter, K., J. Woodward, N. Ross, S. A. Dunning, R. G. Bingham, H. F. J. Corr, and M. J. Siegert (2015), Airborne radar evidence for tributary flow switching in Institute Ice Stream, West Antarctica: Implications for ice sheet configuration and dynamics, *J. Geophys. Res. Earth Surf.*, *120*, 1611–1625, doi:10.1002/2015JF003518.

Wolstencroft, M., et al. (2015), Uplift rates from a new high-density GPS network in Palmer Land indicate significant late Holocene ice loss in the southwestern Weddell Sea, *Geophys. J. Int.*, *203*, 737–754, doi:10.1093/gji/ggv327.

Wright, A. P., et al. (2014), Sensitivity of the Weddell Sea sector ice streams to sub-shelf melting and surface accumulation, *Cryosphere*, *8*(6), 2119–2134, doi:10.5194/tc-8-2119-2014.